BACHELOR THESIS & COLLOQUIUM - ME 141502

INTEGRATION OF AN ENERGY STORAGE IN CONNECTION WITH THE COMBUSTION CHAMBER OF A DIESEL ENGINE TO REDUCE THE NOX EMISSION.

DION ARMAN LILIPALY

NRP. 04211441000004

SUPERVISORS:

Prof. Dr.-Ing. Karsten Wehner

M.Sc. Steffen Loest

DOUBLE DEGREE PROGRAM
MARINE ENGINEERING DEPARTMENT
FACULTY OF MARINE TECHNOLOGY
INSTITUT TEKNOLOGI SEPULUH NOPEMBER
SURABAYA 2018

BACHELOR THESIS – ME 141502

INTEGRATION OF AN ENERGY STORAGE IN CONNECTION WITH THE COMBUSTION CHAMBER OF A DIESEL ENGINE TO REDUCE THE NOX EMISSION

Dion Arman Lilipaly
NRP. 04211441000004

Supervisor:
Prof. Dr.-Ing Karsten Wehner

Co-Supervisor:
M.Sc. Steffen Loest

DOUBLE DEGREE PROGRAM OF
MARINE ENGINEERING DEPARTMENT
FACULTY OF MARINE TECHNOLOGY
INSTITUT TEKNOLOGI SEPULUH NOPEMBER
SURABAYA
2018

APPROVAL FORM

INTEGRATION OF AN ENERGY STORAGE IN CONNECTION WITH THE COMBUSTION CHAMBER OF A DIESEL ENGINE TO REDUCE THE NOx EMISSION

BACHELOR THESIS

Submitted to Comply One of the Requirement to obtain a Bachelor of Engineering
in
Department of Marine Engineering
Faculty of Marine Technology
Institut Teknologi Sepuluh Nopember
Surabaya

Prepared By

DION ARMAN LILIPALY
NRP. 04211441000004

Approved By 1st Supervisor and 2nd Supervisor:

1. Prof. Dr.-Ing K. Wehner ( )

2. MSc. S. Loest ( )

Rostock, July 2018

"This page intentionally left blank"

APPROVAL FORM

INTEGRATION OF AN ENERGY STORAGE IN CONNECTION WITH THE COMBUSTION CHAMBER OF A DIESEL ENGINE TO REDUCE THE NOx EMISSION

BACHELOR THESIS

Submitted to Comply One of the Requirement to obtain a Bachelor of Engineering
in
Department of Marine Engineering
Faculty of Marine Technology
Institut Teknologi Sepuluh Nopember
Surabaya

Prepared By

DION ARMAN LILIPALY
NRP. 04211441000004

Approved by
Head of Marine Engineering Department

Dr. Eng. M. Badrus Zaman, S.T., M.T.
NIP. 1977 0802 2008 01 1007

SURABAYA
AUGUST, 2018

"This page intentionally left blank"

DECLARATION OF HONOR

I hereby declared that:

This final project report has written without any plagiarism act, and confirm consciously that all the data, concepts, design, references, and material in this report own by Hochschule Wismar department of Maritime Studies which are the product of research study and reserve the right to use for further research study and its development.

Name	:	Dion Arman Lilipaly
NRP	:	0421441000004
Bachelor Thesis Title	:	INTEGRATION OF AN ENERGY STORAGE IN CONNECTION WITH THE COMBUSTION CHAMBER OF A DIESEL ENGINE TO REDUCE THE NOX EMISSION.
Department	:	Double Degree Program of Marine Engineering

If there is plagiarism act in the future, I will fully responsible and receive the penalty that will be given by ITS and Hochschule Wismar according to the regulation applied.

Surabaya, August 2018

Dion Arman Lilipaly

"This page intentionally left blank"

INTEGRATION OF AN ENERGY STORAGE IN CONNECTION WITH THE COMBUSTION CHAMBER OF A DIESEL ENGINE TO REDUCE THE NOx EMISSION.

Name : **Dion Arman Lilipaly**

NRP : **0421441000004**

Department : **Double Degree Program of Marine Engineering**

Supervisor : **Prof. Dr.-Ing. Karsten Wehner**

M.Sc. Steffen Loest

ABSTRACT

This thesis is focusing on how to reduce the NOx emission since it has been an issue in all over the world. An idea that reduced the combustion temperature by integrating an external chamber connected with the combustion chamber as a temporary energy storage. This method is implementing the pressure-temperature law, where the pressure is reduced by expanding the volume that resulted a temperature decreased. The aims of this study were to make a feasibility study of the previous invention, a combustion model simulation and technical drawings design of the external chamber. The simulation model involves an analysis of how the temporary energy stored effected the combustion temperature and calculating the pipeline losses. The results showed that by installing the external chamber, the combustion temperature was reduced significantly by 6.15% for the burn zone and 17.8% for the unburn zone. Furthermore, a comparison of the pipeline heat loss showed that an insulated pipe saved 94.1% more heat energy than the uninsulated. The important factor in designing the external chamber were the spring deflection and piston bore. An analysis shown that the larger the deflection and piston bore, the bigger the pressure drop would be which is why an optimization of those factors were needed.

PENGINTEGRASIAN PENYIMPAN ENERGI YANG TERKONEKSI DENGAN RUANG BAKAR DARI MESIN DIESEL UNTUK MENGURANGI EMISI NOx

Nama : Dion Arman Lilipaly

NRP : 0421441000004

Departemen : Double Degree Program of Marine Engineering

Supervisor : Prof. Dr.-Ing. Karsten Wehner

M.Sc. Steffen Loest

ABSTRACT

Thesis ini berfokus dalam cara mengurangi emisi NOx, yang sidah menjadi masalah di seluruh negara. Sebuah metode baru dengan mengurangi temperature pembakaran dengan mengintegrasikan sebuah penyimpan energi sementara yang terkoneksi langsung dengan ruang bakar. Metode ini menggunnakan *pressure-temperature law*, dimana tekanan akan menurun apabila volume diperbesar yang mengakibatkan penurunan temperatur. Pembahasan dari penelitian ini adalah menganalisa patent atau ide yang telah dibuat oleh para penemu sebelumnya, membuat model *combustion simulation* dengan menggunakan metode *two-zone combustion* dan desain 3D dari penyimpan energi yang bernama *secondary chamber*. Dalam model simulasi ini terdapat analasi effek bagaimana energi yang tersimpan dalam *secondary chamber* dapat mempengaruhi temperature pembakaran dan menghitung *losses* yang terjadi di pipa koneksi antara ruang bakar dan *secondary chamber*. Hasil menunjukkan bahwa temperature pembakaran menurun secara signifikan sebesar 6.15% untuk *burn zone* dan 17.8% untuk *unburn zone*. Kemudian sebuah komparasi *heat losses* antara pipa yang menggunakan insulasi dan tanpa insulasi menunjukkan bahwa insulasi dapat menyimpan energi panas lebih banyak sebesar 94.1% dibandingkan tanpa insulasi. Dan faktor terpenting dalam mendesain *secondary chamber* adalah pengaturan defleksi pegas dan diameter piston didalamnya. Hasil analisi menunjukkan bahwa semakin besar defleksi pegas dan diameter piston maka semakin besar *pressure drop* yang terjadi, oleh karena itu proses optimisasi sangat diperlukan.

PREFACE

This Bachelor Thesis is submitted to fulfil the final requirement to obtain the Bachelor of Engineering Degree in Department of Marine Engineering, Sepuluh Nopember Institute of Technology and Hochschule Wismar.

First of all, I would like to thank God for his blessing and giving me the knowledge and opportunity to complete my bachelor thesis in Germany. I would like to express my gratitude to my supervisors Prof. Dr. -Ing. K. Wehner and MSc. S. Loest, who gave me a lot of advice, support and guidance to complete this thesis. Also, Mr. Herlan for giving me the basic knowledge of software design, and all of my friends and senior who helped me settled during my stay in Germany.

The greatest appreciation would be dedicated to my parents and family for their support and motivation. Lastly, I would like to thank my fellow class of 2014 Marine Engineering Students for being a great friend during my study in ITS.

Surabaya, August 2018

Writer

"This page intentionally left blank"

TASK OF BACHELOR THESIS

Theme: **Integration of an energy storage in connection with the combustion chamber of a diesel engine to reduce the NOx emission**

Student: **Dion Arman Lilipaly**

Supervising Professor:	Prof. Dr. -Ing. K. Wehner	Hochschule Wismar
Assistant Supervisor:	MSc. S. Loest	Hochschule Wismar

Date of issue: April 2018
Filling Date: July 2018

The exhaust gas emissions, especially the emissions of NOx and Soot must be minimized for all diesel processes. The causes for the forming of these emission are the non-homogenous mixture between air and fuel during injection and the very high combustion temperatures in special areas of the combustion chamber. For the reduction of the emission, the temperature during the combustion process must be reduced. For this purpose, a storage is to be constructed which temporarily stores energy during combustion and releases it again with a time delay.

The following aspects should be particularly considered:

1. Feasibility study of the spring based connecting rod, Flexible Connecting Rod
2. Calculation of the amount of gas volume and energy that needs to be reduced in order to lower the combustion temperature.
3. Calculation and design the dimension of the energy storage.
4. Dimension and the specification of the spring inside the energy storage.
5. Calculation of the losses inside the energy storage pipeline.

The supervising Professor reserves the rights to extend or to narrow down the scope of the task during processing. Establishing contacts with other institutions and companies must be agreed with the supervisors. The publication of the work or parts of it requires the prior permission of the supervisor. The work shall be prepared in accordance with the applicable guidelines of Hochschule Wismar for academic and scientific work. At least two consultations with the supervising Professor are required as part of the processing. The finished work is to be submitted in electronic form and in four printed copies in the organization office in Warnemünde.

_____
Prof. Dr. -Ing. K. Wehner

TABLE OF CONTENTS

APPROVAL FORM i
DECLARATION OF HONOR iii
ABSTRACT iv
PREFACE vi
TASK OF BACHELOR THESIS vii
TABLE OF CONTENTS viii
LIST OF FIGURES xi
LIST OF TABLES xiii
LIST OF ABBREVIATIONS xv
CHAPTER I 1
I.1 Background 1
I.2 Statement of Problems 2
I.3 Research Limitation 2
I.4 Research Objectives 2
I.5 Research Benefits 2
CHAPTER II 3
II.1 Engine Kinematic Movements 4
II.2 Combustion 5
II.2.1 Two Zone Combustion 5
II.2.2 Burn and Unburn Mass Fraction 6
II.2.3 Burn and Unburn Temperature 6
II.2.4 Mechanical Work 7
II.1.5 Heat Transfer in Cylinder Liner 7
II.2.6 Heat Release 8
II.2.7 Internal Energy 8
II.3 Spring 9
II.3.1 Considerations in Spring Design 9
II.3.2 Helical Spring 11

CHAPTER III 15
III.1 Methodology Flowchart 16
III.2 Definition of Methodology Flowchart 17
III.2.1 Statement of Problems 17
III.2.2 Literature Study 17
III.2.3 Collecting Data 17
III.2.4 Feasibility Study 17
III.2.5 Calculation of Gas Volume 18
III.2.6 Calculation of Losses in Pipeline 18
III.2.7 Design of External Chamber 18
III.2.8 Spring Optimization 18
CHAPTER IV 19
IV.1 Feasibility Study 19
IV.1.1 Spring based Connecting Rod 19
IV.1.2 C Connecting Rod 21
IV.1.3 S Connecting Rod 22
IV.1.4 Additional Chamber 23
IV.2 Calculation of Gas Volume and Energy 24
IV.2.1 Engine Specification 24
IV.2.2 Measurement Data 25
IV.2.3 Compression Pressure and Cylinder Volume 26
IV.2.5 Burn and Unburn Temperature 27
IV.2.6 Internal Energy 29
IV.2.7 Secondary Chamber 31
IV.2.7.5 New Cylinder Pressure 36
IV.2.8 Burn and Unburn Temperature Comparison 37
IV.3 Design of The Energy Storage 39
IV.4 Spring Design 46
IV.5 Pipeline Losses 48
CHAPTER V 57

Bibliography:....58
AUTHOR BIODATA....60
Statement of Authorship....61
Appendix A....1
Appendix B....1
Appendix C....1

LIST OF FIGURES

Figure II.1.1 Engine Geometric....4
Figure II.2.1.1 Two Zone Combustion Model....5
Figure II.3.1. Mechanical Spring....9
Figure II.3.2.1 Helical Spring Design....11
Figure III.1.1 Methodology Flowchart....16
Figure IV.1.1.1. Spring based connecting rod....19
Figure IV.1.2.1. C Connecting Rod....22
Figure IV.1.3.1 Infiniti VC-T....23
Figure IV.2.3.1 Cylinder Pressure....25
Figure IV.2.3.2 Heat Transfer Coefficient....25
Figure IV.2.4.1 Cylinder Volume....26
Figure IV.2.4.2 Compression Pressure....26
Figure IV.2.5.1 Burn and Unburn Mass....27
Figure IV.2.5.2 T burn, T unburn and T mix....28
Figure IV.2.6.1 Heat Transfer....29
Figure IV.2.6.2 Heat Release....29
Figure IV.2.6.3 Mechanical Work....30
Figure IV.2.6.4 Internal Energy....30
Figure IV.2.7.1.1 Secondary Chamber....31
Figure IV.2.7.3.1 Cylinder Pressure Simulation....33
Figure IV.2.7.4.1 Spring Deflection....34
Figure IV.2.7.4.2 Spring Work over Deflection....35
Figure IV.2.7.4.3 Spring Work over Crank Angle....35
Figure IV.2.7.4.4 Energy Stored....36
Figure IV.2.7.5.1 Cylinder Pressure Comparison....37
Figure IV.2.8.1 Burn Temperature Comparison....38
Figure IV.2.8.2 Unburn Temperature Comparison....38
Figure IV.2.8.3 Mix Temperature Comparison....39
Figure IV.3.1 Energy Storage Design....40

Figure IV.3.2 Piston 100 mm....41
Figure IV.3.3 Piston 120 mm....42
Figure IV.3.4 Liner 100 mm....43
Figure IV.3.5 Liner 120 mm....44
Figure IV.3.6 Bottom Part of The Secondary Chamber....45
Figure IV.4.1 Spring 1 Deflection....48
Figure IV.4.2 Spring 2 Deflection....48
Figure IV.5.1 External Chamber System....48
Figure IV.5.2 Pressure Drop per Crank Angle....51
Figure IV.5.3 Pipeline Dimension....52
Figure IV.5.3 Heat Loss Comparison....56

LIST OF TABLES

Table II.1.4.1 A value 7
Table II.2.1.2 Key points of spring design based on 10
Table IV.1.1.1 Spring Design Parameter 20
Table IV.1.1.2 Spring Design Pressure 20
Table IV.1.1.3 Spring Design Requirement 20
Table IV.1.1.4 Spring Dimension 21
Table IV.2.2.1 Engine Specification 24
Table IV.2.7.2.1 Minimum and Maximum Working Load 32
Table IV.2.7.2.1 Minimum and Maximum Working Load 32
Table IV.2.7.3.1 Secondary Chamber Specification 33
Table IV.3.1 Ceramic Properties 40
Table IV.3.2 Piston Specification 41
Table IV.3.3 Liner Specification 42
Table IV.3.4 Aluminum Alloy Properties 44
Table IV.3.5 Bottom Specification 45
Table IV.4.1 Non-Linear Optimization 46
Table IV.4.2 Piston Area 46
Table IV.4.3 Spring Material 46
Table IV.4.4 Spring Geometry Design 47
Table IV.5.1 Pipe and Calculation Information 49
Table IV.5.2 Major Loss Calculation Example 50
Table IV.5.3 Static Loss Calculation Example 50
Table IV.5.4 List of Fittings 50
Table IV.5.5 Minor Loss Calculation Example 51
Table IV.5.6 Minor Loss Calculation Example 51
Table IV.5.7 Heat Loss Calculation Data 53
Table IV.5.8 Pipe and Fluid Specification 53
Table IV.5.9 Thermal Resistance of the fluid and pipe 54
Table IV.5.10 Outside Air Heat Transfer Coefficient 55

Table IV.5.10 Outside Air Heat Transfer Coefficient 55

LIST OF ABBREVIATIONS

Vc	= Volume Clearance (m^3)
Vd	= Volume Displacement (m^3)
B	= Bore (m)
L	= Stroke (m)
S	= Piston Movement (m)
lr	= Connecting Rod Length (m)
a	= Crank Radius (m)
TDC	= Top Dead Center
BDC	= Bottom Dead Center
SI	= Spark Ignition
CI	= Compression Ignition
S	= Piston Travel Distance
V_c	= Clearance Volume
V_d	= Displacement Volume
λ_{pl}	= Connecting Rod Ratio
Ɛ	= Compression Ratio
1	= Burn Zone
2	= Unburn Zone
m	= mass (kg)
P	= Pressure (Pa)
φ	= Crank Angle Degree (°)
φ_{SOC}	= Start of Combustion (°)
φ_{EOC}	= End of Combustion (°)
$\Delta\varphi_{CD}$	= Combustion Duration
X_b	= Mass Fraction Burned
W	= Mechanical Work (J)
Q_w	= Heat Transfer in Cylinder (J)
T_w	= Wall Temperature (K)
T_{gas}	= Gas Temperature (K)
A_{liner}	= Combustion Chamber Area (m^2)
,1	= Pre-mixed Area
,2	= Mixed Area
NCV	= Net Calorific Value (kJ/kg)
m_{fuel}	= Fuel mass (kg)
C_p	= Specific Heat of Gas (kJ/kg.K)
C_v	= Specific Heat of Gas (kJ/kg.K)
R_1	= Individual Gas Constant Burn Area (kJ/kg.K)

R_2 = Individual Gas Constant Unburn Area (kJ/kg.K)
Q_f = Heat Release (J)
δ = Deflection (mm)
w = Load (N or kN)
k = Stiffness (N/mm)
G = Modulus of rigidity (N/mm^2)
n = Number of active coils
n′ = total number of coils
c = Spring index
D = Mean coil diameter (mm)
d = wire diameter (mm)
Ks = Wahl safety factor
Kw = Wahl correction factor
P = Pitch of spring (mm)
Ls = Solid Length (mm)
Lf = Free length (mm)
V = Volume of spring (mm3)
$P_{major\ loss}$ = Major Pressure Loss (bar)
λ = Friction Factor
ρ = Density (kg/m^3)
L = Length of the Pipeline (m)
D = Diameter of the Pipe (m)
Re = Reynold Number
μ = Viscosity (m^2/s)
T = Temperature (K)
h = Height between Suction and Discharge Point (m)
ΣK = Total throughout the Pipeline.
h_f = Minor Loss (bar)
v = Velocity (m/s)
g = Gravity (m/s^2)
Q_{loss} = Heat Loss (kJ)
T_i = Fluid Temperature (K)
T_o = Surface Temperature (K)
R_t = Thermal Resistance
R1 = Inner Radius of the Pipe (m)
R2 = Outer Radius of the Pipe (m)
R3 = Radius of the Insulation (m)
σ = Stefan Boltzmann Constant (W/m^2.K)
Ɛ = Emissivity of the Material

Nu	= Nusselt Number
Ra	= Rayleigh Number
Pr	= Prandtl Number
Gr	= Grashof Number
β	= Coefficient of Fluid Volume Expansion

CHAPTER I
INTRODUCTION

I.1 Background

Global warming is a huge problem for all of the nation. Every country has its own way or policy to prevent the climate change to get worse, for instance the U.S has its own environmental protection agency and European Union has their Euro Standard. According to Mckinsey, the annual worldwide automotive growth from 2012 till 2020 is 6 percent. And most of them still used an internal combustion engine as their prime mover. Diesel engine is one of the IC engine that was very popular to used.

Diesel engine is a very common type of engine that used in many kind of industries, such as, transportation and power plant. High thermal efficiency and also durability are the reasons why they choose this internal combustion engine. However, due to high compression that led to high temperature combustion resulted a chemical process that produce NOx emission. Furthermore, a short time of combustion led to incomplete combustion that resulted a soot particle which is very dangerous to human health and environment.

Nitrogen Oxides (NOx) is a highly reactive gas, which consist of nitrogen and oxygen in a chemical bond. Commonly, NOx is resulted from a high temperature combustion. Nevertheless, there are 3 opportunities for NOx to form, thermal NOx, fuel NOx, and prompt NOx. Meanwhile, soot is a black carbon particle, which has a dimension of 2.5 micrometers that resulted from an incomplete combustion. According to environmental protection agency of the U.S, there are many ways to reduce those two pollutions.

In this thesis, a modification to the combustion chamber by adding an energy storage consist of a spring and additional chamber, will eventually reduce the peak pressure of the combustion and also increase the combustion time that led to the decrease of NOx and Soot emission. Hence, the additional chamber will be built and installed directly into the engine. However, there are still considerations in the energy storage especially, the volume and the spring dimension.

I.2 Statement of Problems

Based on the description above the problems of this thesis are:

1. How to do a feasibility study of Spring based connecting rod, C connecting rod and S connecting rod?
2. How to calculate the amount of gas volume and energy to keep the combustion temperature lower than initial condition?
3. How to calculate the additional chamber dimension?
4. How to calculate the spring dimension inside the additional chamber?
5. How to calculate the losses inside the additional chamber pipeline?

I.3 Research Limitation

The limitations of this thesis are:

1. This thesis is focusing on the temperature of the combustion.
2. Efficiency and power of the engine are not considered.
3. The engine that used for the research is a 1-cylinder engine.
4. The result of this thesis is the volume of the energy storage, geometry of the spring and design of the secondary chamber.

I.4 Research Objectives

The objectives of this thesis are:

1. To know the principle of the Spring based connecting rod, C and S connecting rod.
2. To calculate the amount of gas volume to keep the combustion temperature below initial condition.
3. To calculate the additional chamber dimension.
4. To calculate the spring dimension inside the additional chamber.
5. To calculate the losses inside the pipeline.

I.5 Research Benefits

The benefits of this thesis are:

1. Minimizing the pollution that cause by the internal combustion en

CHAPTER II
STUDY LITERATURE

Internal Combustion Engine requires lean fuel-air mixture in order to produce adequate combustion for the power stroke. Engine performance is very important to be monitored for instance Power and rpm. However, the engine performance determines by the combustion process inside the engine. Combustion is a process that involves fuel, air and temperature, at certain condition those mixtures will ignite and produces a force. The pressure from the combustion's force will be measure over the crank angle. Direct measurement requires cylinder pressure sensing equipment (Heywood, 1988). Consequently, due to high compression combustion especially diesel engine, the emissions from the combustion such as NOx and soot were produced simultaneously from the high temperature and imperfect chemical reaction.

There are several ways to reduce the hazardous emission from the diesel engine. The techniques can be classified into three categories, fuel change, combustion engineering and exhaust gas treatment. In this thesis, the engine's combustion will be engineered by reducing the peak pressure. Therefore, the combustion temperature will simultaneously reduce as well. An energy storage consist of spring will be installed in the additional chamber. The spring has a function to control the volume of combustion chamber, as spring has a characteristic to store energy and release it later.

II.1 Engine Kinematic Movements

The engine kinematics movement consist of different variables that can be solved by using the engine geometry. As one variables can influence one another, hence a deep knowledge of engine geometry is imperative. The figure down below illustrates the engine geometry that needed to solve the engine kinematics movement.

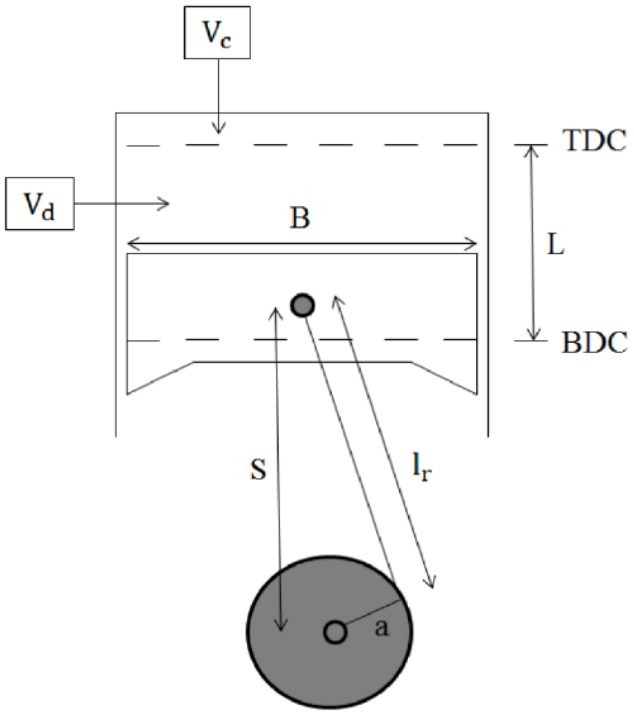

Figure II.1.1 Engine Geometric

Source: Gde's Master Thesis

From the figure above can be described that the engine kinematic movement are solved by using engine geometry, as explain by the equation below.

Clearance Volume (TDC)

$$v_c = \frac{v_d}{(C_r - 1)} . No. Cylinder \ldots (2.1)$$

Displacement Volume

$$v_d = No. Cylinder \, . A_{piston} . L \ldots (2.2)$$

Connecting Rod Ratio

$$\lambda_{pl} = \frac{L}{2 \, .lr} \ldots (2.3)$$

Crank Angle Radius

$$a = \frac{L}{2} \dots (2.4)$$

Cylinder Volume

$$Vol. = V_{TDC} + \frac{(D^2.\pi.s(\varphi))}{4} \dots (2.5)$$

Piston Travel

$$s(\varphi) = a\,.\,(1 - \cos(\varphi) + \left(\frac{\lambda_{pl}}{2}\right).\,sin^2(\varphi) \dots (2.6)$$

II.2 Combustion

II.2.1 Two Zone Combustion

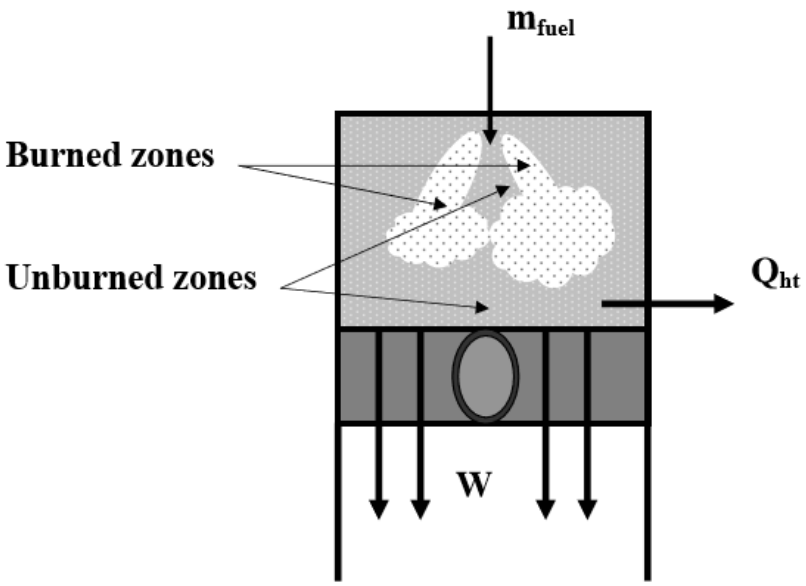

Figure II.2.1.1 Two Zone Combustion Model

Source: me.ud.edu

In two zone model, the environment inside the combustion chamber are assume consist of two zones, the burned zone and the unburned zone. The two zones are utilizing the thermodynamic (First Law of Thermodynamics) systems with energy and mass interactions between themselves and their common surroundings, the cylinder walls. By using this model, the in-cylinder pressure as a function of crank angle can be assumed from energy release or burned profile.

$$V_1 + V_2 = V(\varphi) \dots (2.7)$$

$$m_1 + m_2 = m(\varphi) \dots (2.8)$$

$$p_1 = p_2 = p(\varphi) \text{ ... (2.9)}$$

II.2.2 Burn and Unburn Mass Fraction

Whilst the mass inside the cylinder is known, the fraction combustion chamber gasses can be made into burned and unburned masses. The initial condition of the instantaneous change in mass-fraction burned $\frac{dX_b}{d\varphi}$ is zero.

$$m_1(\varphi) = m_1(\varphi - 1) + \frac{dX_b}{d\varphi}(\varphi)m(\varphi) \text{ ... (2.10)}$$

$$m_2(\varphi) = m_2(\varphi - 1) - \frac{dX_b}{d\varphi}(\varphi)m(\varphi) \text{ ... (2.11)}$$

$$X_b(\varphi) = 1 - \exp[-a\left(\frac{\varphi - \varphi soc}{\Delta\varphi_{CD}}\right)^{k+1}] \text{ ... (2.12)}$$

II.2.3 Burn and Unburn Temperature

The most common way to solve the burned and unburned temperature is by using the ideal gas assumption. The method can be used when the mass, volume, pressure and gas constant are known.

$$T_2(\varphi) = \left(\frac{p(\varphi)V(\varphi)}{m_2(\varphi)R_2}\right) - \frac{\left(\frac{m_1(\varphi).R_1.B(\varphi).A^*}{m_2(\varphi).R_2}\right)}{(1+(\frac{m_1.R_1}{m_{2.}R_2})} \text{ ... (2.13)}$$

$$T_1(\varphi) = \frac{p(\varphi)V_1(\varphi)}{m_1(\varphi)R_1} \text{ ... (2.14)}$$

$$T_{mix} = (\frac{(C_{v1}.m_1.T_1)+(C_{v2}.m_2.T_2)}{(C_{v1}.m_1)+(C_{v2}.m_2)}) \text{ ... (2.15)}$$

There is also another method that was proposed by Heider. There are considerations which lead to the following empirical method for the temperature difference between both of these zones.

$$T_1(\varphi) - T_2(\varphi) = B(\varphi)A^* \text{ ... (2.16)}$$

For the function B(ϕ) is valid. Based on Woschni, B(ϕ) is function which leads the difference between the cylinder pressure p(ϕ) and the theoretical pressure P0(ϕ) is utilized for the consideration of the influence of combustion and A^* describes the temperature level in reaction zones as the start of combustion. Cgl for engines with 4-valve technology and central injection nozzle is 0.15 and for engines with 2-valve technology and a side injection nozzle is 0.07. ʎgl

describes the global air-fuel ratio. λ_0 for small to the medium-sized diesel engine is 1.0 and large diesel engine is 1.03.

$$B(\varphi) = 1 - \frac{\int_{\varphi soc}^{\varphi}[p(\varphi)-p_o(\varphi)]m_1 d\varphi}{\int_{\varphi soc}^{\varphi EOC}[p(\varphi)-p_o(\varphi)]m_1 d\varphi} \ldots (2.17)$$

$$A^* = A\frac{1.2+(\lambda_{gl}-1.2)^{Cgl}}{2.2\lambda_0} \ldots (2.18)$$

A stands for engine specific factor that depends on the engine itself. The amount of A can be determined from the table II.1 below. With $\lambda_0 = \lambda_{gl}$ and A^* = *constant*.

Table II.1.4.1 A value

Engine					
Bore [mm]	Stroke [mm]	Cycle	Compression ratio	rated speed	A value [K]
79.5	95.5	4	19.5	4000	1650
128	142	4	16	2100	1740
160	180	4	14	1500	1580
480	600	4	14	450	1650
580	1700	2	17	127	1655

II.2.4 Mechanical Work

The mechanic work is the output energy from the piston that can be calculated while the pressure and cylinder volume changes are determined.

$$\frac{dW}{dt} = -P\frac{dV}{dt} = -P\omega\frac{dV}{d\varphi} \ldots (2.19)$$

II.1.5 Heat Transfer in Cylinder Liner

Heat transfer consist of conduction, convection and radiation. Sometimes the radiation (dQ_ε/dt) is added to the convective heat transfer coefficient, although the maxima of (dQ_α/dt) and (dQ_ε/dt) actually appear shifted with reference to the crank angle.

$$\frac{dQ_w}{dt} = \frac{dQ_a}{dt} + \frac{dQ_\varepsilon}{dt} \ldots (2.20)$$

$$\frac{dQ_w}{dt} = \Sigma_i \alpha_i A_i (T_{w,i} - T_{gas}) \ldots (2.21)$$

The cylinder liner consists of three different things. The cylinder head, piston and also the liner itself.

$$A_{liner} = A_{chamber} + A_{Piston} + D\pi s(\varphi) \dots (2.22)$$

$$A_{chamber} = 2\,.\,A_{Piston} \dots (2.23)$$

II.2.6 Heat Release

Heat release is the energy that resulted from the combustion process in a form of heat. To calculate it, most diesel engine use double vibe function. This method divided the combustion period into two are, premixed area and mixed area.

$$Q_{ftotal} = m_{fuel}\,.\,NCV_{fuel} \dots (2.24)$$

$$\frac{dQ_{f,1}}{d_\varphi} = 17.2\,(6.908\,.\left(\frac{Q_{ftotal}\,.0.6}{\Delta\varphi_{CD,1}}\right).(m_1+1).\left(\frac{\varphi-\varphi_{soc,1}}{\Delta\varphi_{CD,1}}\right)^{m_1}.e^{-6.908\left(\frac{\varphi-\varphi_{soc,1}}{\Delta\varphi_{CD,1}}\right)^{m_{1+1}}})\dots (2.25)$$

$$\frac{dQ_{f,2}}{d_\varphi} = 6.2\,.\left(\frac{Q_{ftotal}\,.(1-0.6)}{\Delta\varphi_{CD,1}}\right).(m_2+1).\left(\frac{\varphi-\varphi_{soc,2}}{\Delta\varphi_{CD,2}}\right)^{m_2}.e^{-a\left(\frac{\varphi-\varphi_{soc,2}}{\Delta\varphi_{CD,2}}\right)^{m_{2+1}}} \dots (2.26)$$

with $\varphi_{soc,1} \le \varphi \le (\varphi_{soc,1} + \Delta\varphi_{CD,1})$, $\varphi_{soc,2} \le \varphi \le (\varphi_{soc,2} + \Delta\varphi_{CD,2})$

$$\frac{dQ_f}{d_\varphi} = \frac{dQ_{f,1}}{d_\varphi} = \frac{dQ_{f,2}}{d_\varphi} \dots (2.27)$$

II.2.7 Internal Energy

The internal energy is the energy that related to the pressure, temperature, gas composition and the heat losses. When all of the parameters have been obtained, the internal energy can be determined.

$$\frac{dU}{dt} = \frac{dQ_w}{dt} - \frac{dw}{d_t} + \frac{dQ_f}{d_t} + (H_{in} - H_{out}) \dots (2.28)$$

II.3 Spring

Figure II.3.1. Mechanical Spring

Source: Industrial Spring

A mechanical spring can be defined as an elastic body whose primary function is to deflect or distort under load and which recovers its original shape when released after being distorted (Wahl, 1944). Figure II.1.1 shows the form of helical spring. Every spring has its own characteristic including the range of force or pressure that the spring can handle.

II.3.1 Considerations in Spring Design

The material and the geometry of the spring is very important to fulfil the required pressure. Wahl (1944, p.2) stated that spring have several primary functions:

1. To absorb energy and mitigate shock.
2. To apply a definite or torque.
3. To support moving masses or to isolate vibration.
4. To indicate or control load or torque.
5. To provide and elastic pivot or guide.

Because springs usually deflect by a considerable degree for a given load, it follows relatively large amount of energy must be stored when the springs is in the deflected position. Since both the deflection and load for most springs are proportional to stress and energy is proportional to deflection times load, it follows that in general amount of energy which may be stored is proportional to the *square* of the stress. The most widely used material for springs was carbon steel (Wahl, 1944). According to Lee Spring Limited (2017) Key factors affecting material choice for a particular application include:

1. Material Meets the required stress conditions either static or dynamic.
2. Material is capable with its surroundings i.e corrosive environment.
3. Material must be capable of functioning satisfactorily at the required operating temperature.

4. Special requirements such as conductivity, constant modulus, weight restrictions, magnetic limitations, etc.

Spring could suffer under two different kinds off loads. The static load and the variable range of load.

1. Static load

   In many cases, springs are subject to a load or deflection which is constant or repeated but a few times during the life of spring.

2. Variable load

In many spring applications the load does not remain constant but varies with time. For instance, automotive spring.Where springs are subject to relatively few cycles of loading, the permissible working stress may be considerably increased over that allowable for an infinite number. Examples of such springs are those used in certain control mechanism.

Another factor that should keep in mind is that there is always an unavoidable variation in the size of wire or plate used in making springs. The effect of these variations may often be large, especially when it comes to obtaining proper load-deflection characteristics. Another point, there is a *Wahl* safety factor with a minimum value of 1.05 in order for the spring to passed the test. Hence, multilevel optimization is very common for the researcher to determine the right material and geometry of the spring. There were many researchers that have use the multilevel optimization to optimize the design of the spring Fathallah and Bakar (2009), Fathallah and Bakar (2010) and Ristiawan, Soeprajitno, Fathallah (2013). Table II.2.1.2 shows the key points of designing a spring based on Fathallah and Bakar (2009).

Table II.2.1.2 Key points of spring design based on

Source: Optimization of spring design Fathallah and Bakar (2009)

Criteria	**Symbol**
Wire dieameter (mm)	d
Number of active coils	n
Mean spring diameter (mm)	D
Outer spring diameter (mm)	De
Inner spring diameter (mm)	Di
Free spring length (mmm)	Lf
Preloaded installed length (mm)	Li
Fully loaded operating length (mm)	Lo
Theoritic solid length (N)	Lt
Minimum working loading (N)	Fi
Maximum working loading (N)	Fo
Theoritic limit loading (N)	Fs

Criteria	Symbol
Critical spring speed (m sec^{-1})	Vk
Natural spring frequency (Hz)	fn
Developed wire length (mm)	l
Spring constant (N mm^{-1})	k
Spring weight (kg)	m
Permissible torsional stress (Mpa)	τ_A
Static level of safety	
Fatigue strength for the given loading	τ_{max}

Ristiawan, Soeprajitno and Fathallah (2013) used a Yamaha RS 100 for the simulation. The engine specification was 1 cylinder, 2 stroke linear engine with spring for the return cycle and air cooled. They also used a multilevel approach as the methodology. However, the optimization was done by using a solver function from the Microsoft excel. As a result of the optimization, the chosen spring was the lightest and also had Wahl a safety factor more than 1.05.

II.3.2 Helical Spring

Helical spring is a device that can store energy and release it later instantaneously. They are made from elastic materials that formed into a helix shape. Figure II.1.2.1 describe the helical spring based on the dimensions.

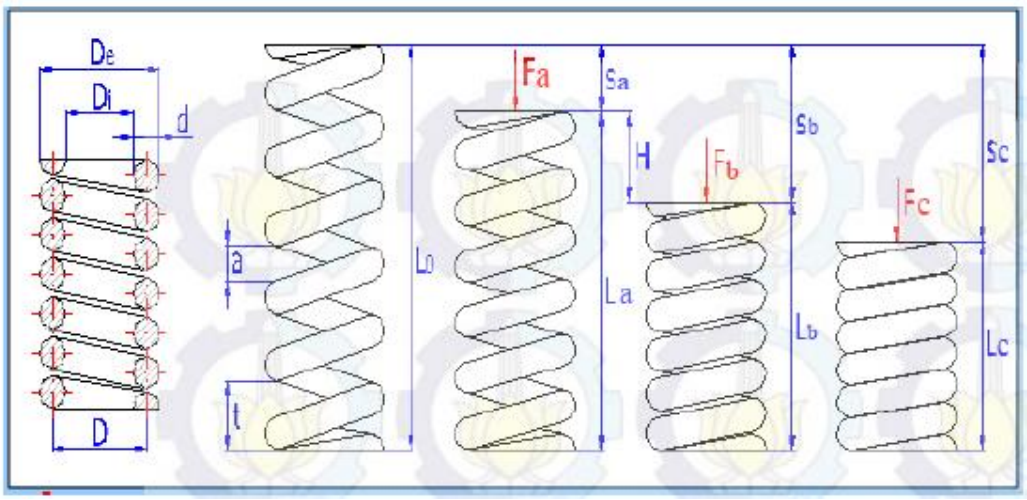

Figure II.3.2.1 Helical Spring Design

Source: Jurnal Teknik Sistem Perkapalan

There are many dimension and equation for designing a spring for instance, spring index, wire diameter, etc. Those factors will varies depend on the load and environment of the springs. However, springs could fail, if one of those

factors were miscalculate. Therefore, down below there will be a detail explanation of the helical springs equation. All of the equation (2.0 till 2.16) were collected from Petele, M. (2017).

II.3.2.1 Spring Index

Ratio of mean coil diameter to material diameter or radial width of cross section for square springs.

$$c = \frac{D}{d} \text{ .... (2.29)}$$

II.3.2.2 Inner Spring Diameter

The inner diameter of the spring is the subtraction of the mean spring diameter by the wire diameter.

$$Di = D - d \text{.... (2.30)}$$

II.3.2.3 Outer Spring Diameter

The outer diameter of the spring is the diameter of the spring that measured from the outer surface of the spring.

$$Di = D + d \text{.... (2.31)}$$

II.3.2.4 Space between coils

The space between each coils of the spring.

$$a = P - d \text{.... (2.32)}$$

II.3.2.5 Pitch

The distance between each downside of the coils.

$$P = a + (Lo - Lc) \text{.... (2.33)}$$

II.3.2.6 Deflection

Deflection is distance moved by spring under the action of certain load whether it's a static load or variable load.

$$\delta = \frac{F}{k} = \frac{8wD^3n}{Gd^4} = \frac{8wc^3n}{Gd} \text{.... (2.34)}$$

II.3.2.7 Spring Stress

The stress that produced by the spring from suffering the working load.

$$\tau b = \frac{8FD}{\pi d^3} \text{.... (2.35)}$$

II.3.2.8 Deflected Spring Length

The length of the spring minus by deflection.

$$L = Lo - \delta \text{.... (2.36)}$$

II.3.2.9 Spring Working Stroke

The length of the spring minus by deflection.

$$H = La - Lb \text{.... (2.37)}$$

II.3.2.10 Wahl Safety Factor

A factor that takes case of both direct shear stress and curvature in springs.

$$Kf = 1 + \frac{1}{2c} \text{.... (2.38)}$$

II.3.2.11 Wahl's Correction Factor

A factor that show how much stronger the spring is to resist the load.

$$Ks = 1 + \frac{0{,}615}{c} \text{.... (2.39)}$$

II.3.2.12 Solid-Length

The length of spring in fully closed condition.

$$Lc = (n + ne)d \text{.... (2.40)}$$

II.3.2.13 Spring Constant

The design spring constant.

$$k = \frac{Gd^4}{8nD^3} \text{.... (2.41)}$$

II.3.2.14 Spring Weight

The mass of the design spring.

$$m = \frac{\pi d^4 \rho l}{4.10^9} \text{.... (2.42)}$$

II.3.2.15 Develop Wire Length

The maximum developed wire length due to temperature.

$$l = 3{,}2.D.(n + 2) \text{.... (2.43)}$$

II.3.2.16 Spring Deformation Energy

The maximum deformation energy that the spring can handle.

$$Wb = \frac{Fb.\delta b}{2000} \ldots. (2.44)$$

CHAPTER III
METHODOLOGY

There are many steps and process that have to be done in order to solve the research problems, the process is called methodology. An engineering design need to go through several optimization and simulation, before It can produce in a prototype model. Hence, a design of energy storage requires certain types of process. The methodology of this thesis is using a software called excel. The data were collected from the previous master thesis that has been done by Gde. Therefore, the engine specification, combustion and emission will be collected.

Furthermore, after the combustion data has been collected, the temperature of the combustion will be analyzed and recalculated in order to keep the combustion temperature as low as possible. From there the amount of gas volume that have to be transfer into the energy storage will be known. After that, the losses calculation inside the energy storage pipeline will be done using the excel software.

The spring will be calculated based on the data collection and optimize by using a multilevel optimization. Multilevel optimization is decomposition technique in which the problem is reformulated as several sub problems (one for each subsystems) and coordination problem (at system level) to preserve the coupling among the sub system (Rao, 1996). According Fathallah and Bakar (2009). Firstly, the pressure from the combustion process must be optimize. After that, the spring geometry will be optimized based on the optimized combustion pressure. And then, dynamic approach will be taken to optimize the spring, hence the spring will deflect for only certain value of pressure.For more detailed workflow of the methodology can be seen in figure III.1.1. Figure III.1.1 explained about the workflow from start till the design of the optimum piston.

III.1 Methodology Flowchart

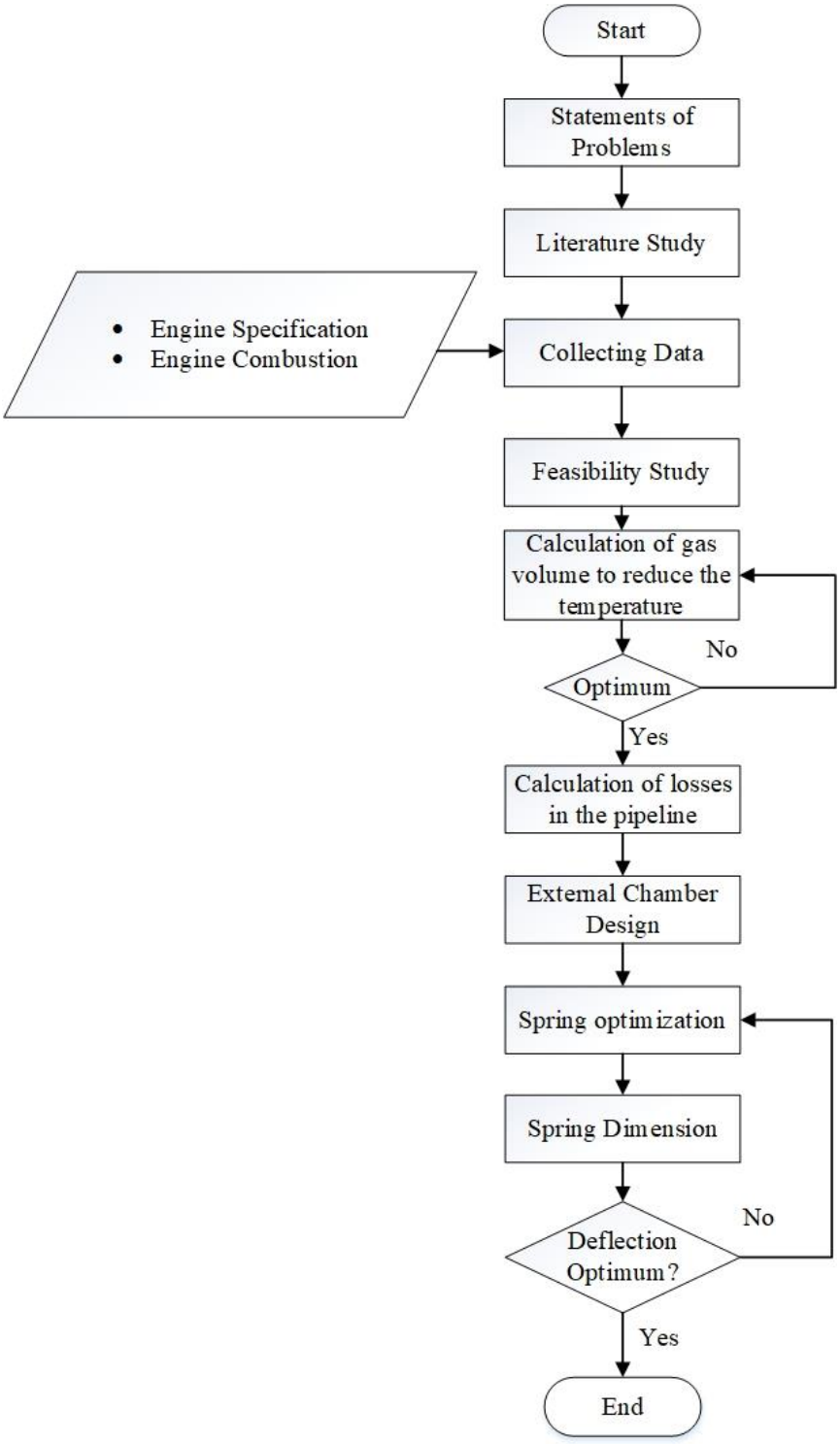

Figure III.1.1 Methodology Flowchart

III.2 Definition of Methodology Flowchart

The flowchart consists of many different stages. Each stage has their own purpose and task. Down below each of the process will be explained in detail.

III.2.1 Statement of Problems

Firstly, in order to find the objectives for the thesis, a process called identifying problems is very necessary. In this stage, the problems of the thesis will be written in question form. From the problems, the objectives of the thesis can be planned. The main purpose of this thesis is to overcome the matter from the statement of problems. To overcome the problems, there will be a literature study and collecting the data information of the problems.

III.2.2 Literature Study

All of the problems that has been identified will be go through a process called literature study. At this stage, various theories from previous researchers that has an influence to the problems will be complied and constructed into a single chapter. Literature study is very important, because It acts as the reference for the research. It can be done by complying the theories from various journals, articles and books.

III.2.3 Collecting Data

In this process, certain information will be collected in order to be studied. The information that has been gathered are the Engine Specification, Combustion. The highest or maximum pressure from the cylinder pressure will be taken and assess for every crank angle.

The engine specification and dimension were collected from the previous research project. And last, the engine's combustion pressure over the crank angle will be gathered from the real simulated data.

III.2.4 Feasibility Study

In this chapter, a brief study will be done regarding the ideas that has been founded by researchers. The working principle will be analyzed and also the advantage and disadvantage of the idea will be summarized and concluded.

III.2.5 Calculation of Gas Volume

The combustion temperature will be reduced as low as possible, by decreasing the combustion pressure. The pressure will be made into constant by adding an additional chamber that will keep the volume of the cylinder + volume of the additional chamber constant over certain crank angles.

III.2.6 Calculation of Losses in Pipeline

After the volume of the additional chamber has been determined, the losses in the pipeline will be calculated. The pressure loss and heat loss will be assessed.

III.2.7 Design of External Chamber

The area and the height of the additional chamber will be determined. This process has a great influence into the spring deflection constraint to keep the volume over crank angle constant.

III.2.8 Spring Optimization

A spring will be used as an energy storage in the additional chamber. From the data collection, the spring design will be optimized to deflect on the designed pressure. The first step of multilevel spring design is optimizing the pressure or force. Every time the spring encounter pressures that exceed the max. allowable pressure, the spring will deflect and expand the volume to reduce the pressure. The second step is geometry optimization, from the optimized force, the geometry of the spring will be optimized. The maximum working loading will be determined from the deviation of the optimum pressure. The spring mass, the static level will be act as the constraint of the geometry optimization. The target will be set to minimum in order to find the lightest weight of spring.

CHAPTER IV
RESULT AND ANALYSIS

IV.1 Feasibility Study

IV.1.1 Spring based Connecting Rod

A mechanical spring is basically an energy storage that store energy via deflection of the spring. The amount of the store energy is depending on the spring constant. The bigger the spring constant the larger amount of energy that the spring can stored. The figure down below gives a description about how the spring can be installed inside the connecting rod.

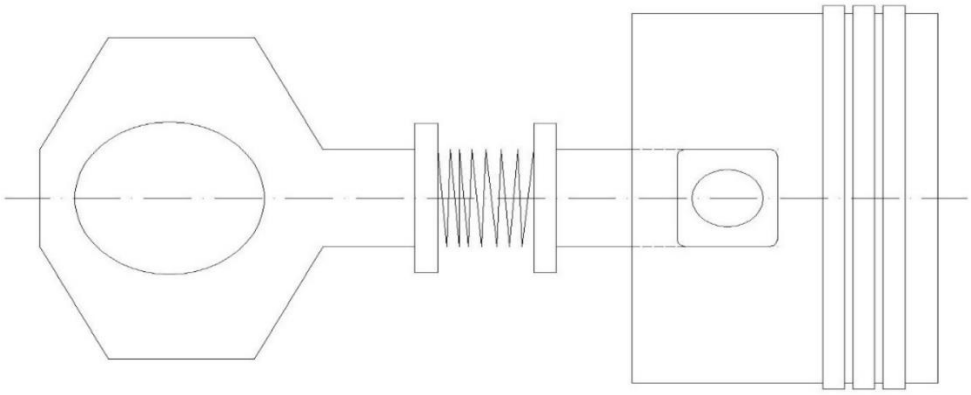

Figure IV.1.1.1. Spring based connecting rod

The purpose of the spring based connecting rod is to reduce the peak pressure of the combustion process, hence from there the temperature will also decreased due to the *pressure-temperature law*. The working principle of this idea is by storing the energy from the combustion process into the spring and release it later when the spring starts to deflect into its initial condition. Therefore, the spring has to be design to be able to withstand the working pressure. Furthermore, the amount of spring deflection has a huge factor to determine how much pressure that spring can reduced in the combustion process.

The advantage of this idea is due to its simple design. In addition, the mechanical spring that will be installed in the connecting rod is easy to be manufactured. Due to its simplicity, this idea does not need any computerized controller to make it work. However, inconsequence of the very high pressure from the combustion, to be able to withstand that amount of pressure the spring dimension has to be very large. And that is the problem of this idea, because the space that the connecting rod provide to installed the spring is very narrow. In

addition, the table down below provide a good feasibility study example of this idea.

Table IV.1.1.1 Spring Design Parameter

Specification Diesel Engine			
Bore	:	150	mm
Stroke	:	180	mm
Cylinder	:	1	
Connecting Rod length	:	332	mm
Space for connecting rod	:	33.2	mm
Speed	:	1500	rpm

The table IV.1.1.1 shows the specification of diesel engine that will be used to implement the idea. The space for connecting rod is assumed 10% from the total length of the connecting rod, hence 33.2 mm is the space that will be provided to installed the spring. From the engine specification can be known that the combustion starts at 358.5° – 470° crank angle. Which means, the peak pressure of the combustion will occur between those crank angle degrees.

Table IV.1.1.2 Spring Design Pressure

	P (bar)	F (N)
Maximum Pressure	109.6	193581
Activation Pressure	98.64	174223
ΔF		19358.1

The table IV.1.1.2 provides the information of the maximum pressure of the combustion which is 109.6 bar. The spring activation pressure is assumed 90% from the max pressure that equals to 98.64 bar. From there, the pressure (bar) has to be converted into force (newton) to calculate the spring dimension.

Table IV.1.1.3 Spring Design Requirement

Spring Design Requirement		
Max. Working Load	193581	N
Min. Working Load	174223	N
ΔF	19358.1	N
Maximum Length	33.2	mm

The spring design requirement provides the constraints for the spring design. The delta F shows the range of force that spring has to withstand. From the data above, the spring design optimization can be started.

Table IV.1.1.4 Spring Dimension

Compression spring		
Number of active coils	n	6
Direction of coil winding	Right	
Spring constant [N/mm]	k	583.0753
Spring weight [kg]	m	5.372
Outer spring diameter	De	123
Inner spring diameter	Di	87
Free spring length	L0	480
Preloaded spring length	L1	181.2
Fully loaded spring length	L8	148
Theoretic spring limit length	L9	144
Minimum working loading [N]	F1	174222.9
Maximum working loading [N]	F8	193581
Theoretic spring limit loading [N]	F9	195913.3
Spring material:		
Chrome-vanadium alloy steel wire JIS SUP 10		
Wire diameter	d	18

After going through optimization process, the smallest spring that able to withstand the maximum pressure are having free length of 480 mm and outer diameter of 123 mm. That is impossible to be installed into the connecting rod, because the space that is provided is only 33.2 mm.

In conclusion, the spring based connecting rod gives a new unconventional way to reduce the combustion temperature, however due to the lack of connecting rod space this idea can be considered as impossible.

IV.1.2 C Connecting Rod

This invention was made to reduce the peak pressure of combustion by adjusting the compression. The basic idea is by making the connecting rod into an elastic form, so that the compression will be depends on the length of it. The challenge of this invention is how to prevent the plastic deformation into exceeding the maximum limit.

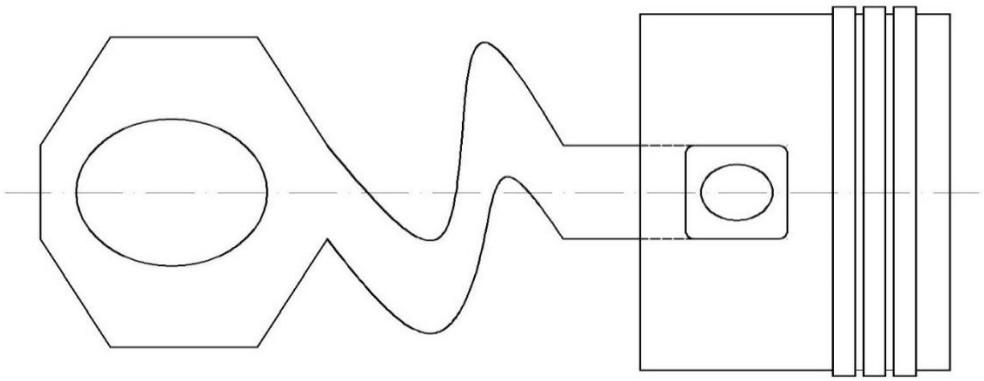

Figure IV.1.2.1. C Connecting Rod

The solution is by adding a support beam on both side that act as a stopper. It will prevent the plastic deformation to exceed beyond the limit. However, there is also another problem in this design, the strength of the longitudinal section is very critical to get a deformation. As a result, a slight bent can be produced from the centrifugal force. Therefore, this solution is only provided an idea or a new method to reduce the combustion pressure.

Additionally, this idea also provides a better option than installing a hydraulic system into the connecting rod that needs a complex system in order to control it. And also, the fast-moving connecting could make the fluid inside the hydraulic chamber to suffer sloshing. This can cause an unstable movement to the connecting rod. Furthermore, the installation of hydraulic chamber into the connecting rod can cause an excessive increase of mass that can lead to the connecting rod strength.

In conclusion, this invention is giving a basic idea about how to reduce the combustion pressure by manipulating the connecting rod length. However, It still need further studies regarding the strength.

IV.1.3 S Connecting Rod

This invention was made by Infiniti, that can simply change the compression ratio from 8:1 to 14:1. The idea behind this invention is to increase the engine efficiency and performance, by adjusting the compression ratio based on the engine load. Basically, this engine needs a Turbocharger to increase its volumetric efficiency. In operation, if the engine is on high load the ECU will adjust the harmonic drive to reduce the compression ratio to avoid knocking. The harmonic drive is using an electric motor that can rotate clockwise or counter-clockwise that can adjust the piston stroke.

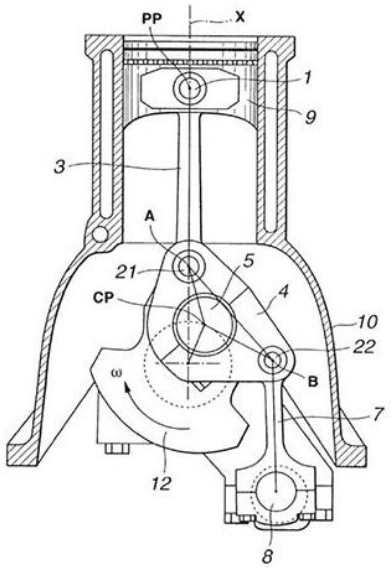

Figure IV.1.3.1 Infiniti VC-T

Source: U.S Patent

Practically, this S connecting rod is only designed for SI engine, Since, CI engine can only work with high compression ratio. Furthermore, the material of the engine could cost cheaper than conventional diesel engine and its multi-link connecting rod could provide central pivoting angle to change its piston stroke effective length. However, due to its dependent on the electric motor that drives the harmonic drive, the long-term reliability of the engine is still question as the failure of the harmonic drive could majorly affect the engine performance and the efficiency.

IV.1.4 Additional Chamber

In 1986, a big automotive company name Volkswagen made a patent (DE3742321A1) about a device compression control. The device is simply an additional chamber that equipped with a spark plug and a piston. The idea behind this invention is to improve the heat dissipation from the combustion process to reduce the NOx emission. Practically, at low loads the additional chamber will have a small volume while, at full load the volume will be the greatest. An electric motor is used for controlling the piston movement inside the additional chamber. However, this invention was never made into mass production by VW.

IV.2 Calculation of Gas Volume and Energy

IV.2.1 Engine Specification

To calculate how much volume and energy that the secondary chamber can store is depending on the engine specification. The table down below is explaining about the diesel engine specification.

Table IV.2.2.1 Engine Specification

Engine Specification			
Bore	=	0.15	m
Stroke	=	0.18	m
Volume Max	=	0.0035	m3
TDC Volume	=	0.00028917	m3
Connecting Rod Ratio	=	0.2711	
Crank Radius	=	0.09	m
Number of Cylinder	=	1	
Compression Ratio	=	12	
Engine Speed	=	1500	RPM
Polytroph	=	1.39	
Scavenge Air Pressure	=	237000	N/m2
		2.37	bar
Engine Specific Factor	=	1550	K
Lambda	=	2.025	
Combustion Start	=	352.25	C.A
Combustion End	=	435.75	C.A
Combustion Duration	=	77.25	C.A
Cp Burn	=	1.113	KJ/Kg.K
Cv Burn	=	0.812	KJ/Kg.K
Cp Unburn (Air)	=	1.005	KJ/Kg.K
Cv Unburn (Air)	=	0.718	KJ/Kg.K
R burn	=	301	KJ/Kg.K
R unburn	=	287	KJ/Kg.K
Supply Start	=	347.25	C.A
Engine Specific Factor Correction	=	2524.569	K
Intake Valve Close	=	205	C.A
Outlet Valve Open	=	470	C.A
Volume TDC	=	0.000289169	m3

The value above will be used to simulate the combustion temperature by dividing it into two zones, the burned and unburned area.

IV.2.2 Measurement Data

The data were measured directly from the engine. Hence, the data are real value. The parameter that are needed for the calculation are the heat transfer coefficient, cylinder pressure, fuel and gas mass. All of those data are only for one load condition (1500 rpm) and each data have a value in each of 0.25 crank angle. The graph down below illustrates the cylinder pressure when the combustion happens.

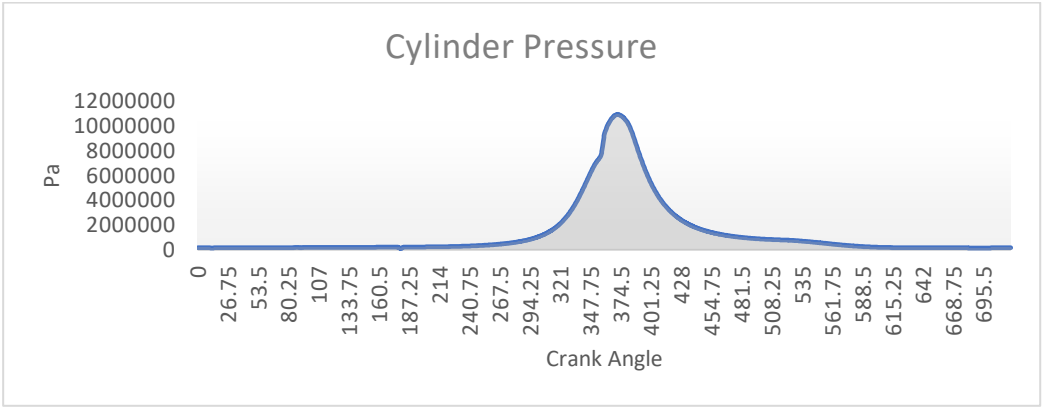

Figure IV.2.3.1 Cylinder Pressure

From the graph can be seen that the peak pressure of the combustion is 109.61 bar. The combustion starts at 352.25 CA and ends at 435.75 CA. Therefore, the peak pressure would have occurred around those two crank angles interval. The graph down below illustrates the heat transfer coefficient per crank angle.

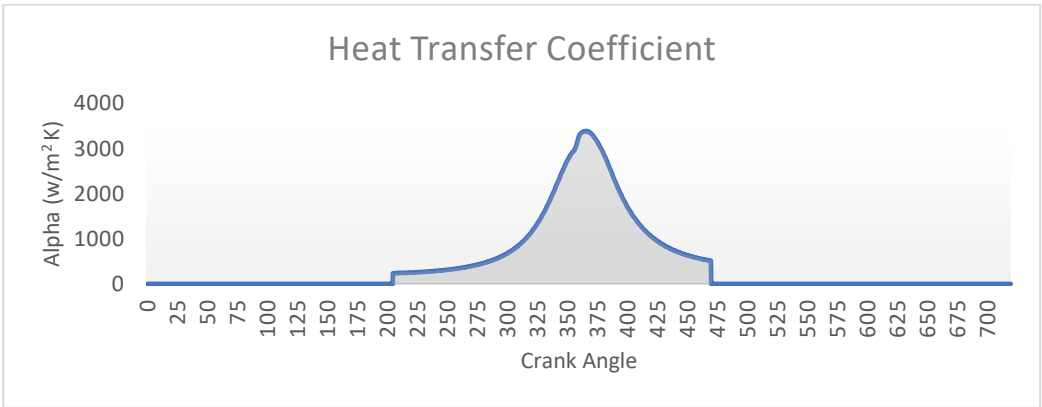

Figure IV.2.3.2 Heat Transfer Coefficient

The heat transfer coefficient began rising when the intake valve closed. That can happen due to the adiabatic process inside the combustion chamber. This coefficient is very important to calculate how much heat energy that were

produced inside the combustion chamber. The bigger the alpha the higher the heat energy will be.

IV.2.3 Compression Pressure and Cylinder Volume

Since the engine is four stroke, hence there will be two peak volume inside the graph. As the four-stroke engine, needs two revolutions in order to complete its process. The figure down below illustrates the value of cylinder volume on each crank angle.

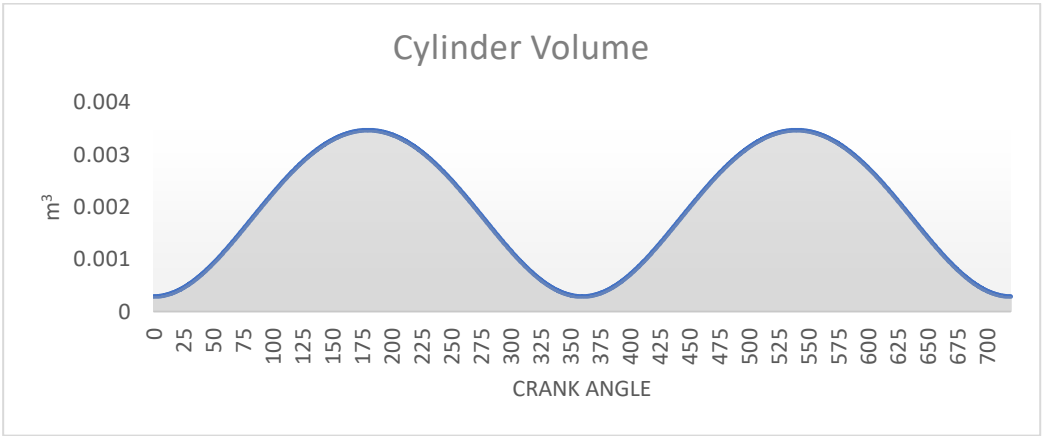

Figure IV.2.4.1 Cylinder Volume

The compression pressure is a condition where the pressure inside the combustion chamber were produced directly from the piston movement. In this condition, the combustion was excluded. The graph down below illustrates the compression pressure inside the engine.

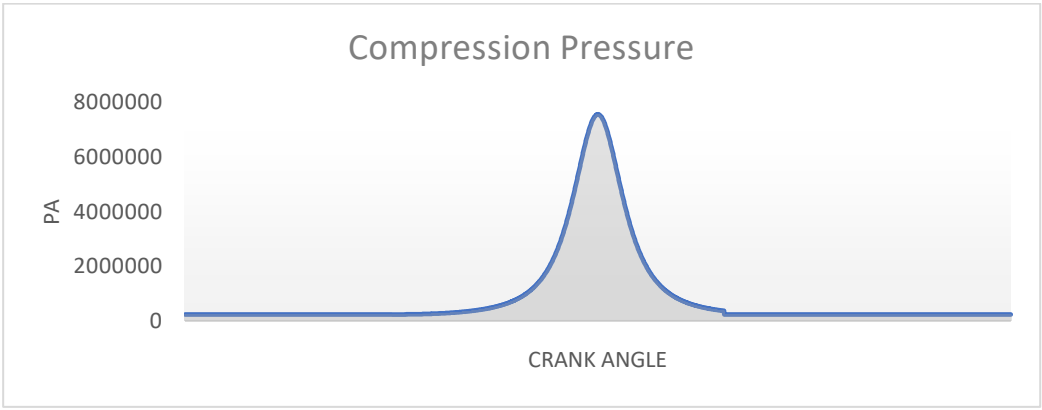

Figure IV.2.4.2 Compression Pressure

IV.2.5 Burn and Unburn Temperature

The combustion is divided into two different zones, the burned and unburn zone. Each of them has its own mass. Hence the temperature is also different. The burned zone is assumed to be the temperature when the combustion happens, while the unburn zone is the temperature around the combustion chamber. Figure II.1.1 illustrates the different between the burned and unburned zone. The calculation starts from determining the burn and unburn mass fraction by using the equation (2.4), (2.5), (2.6).

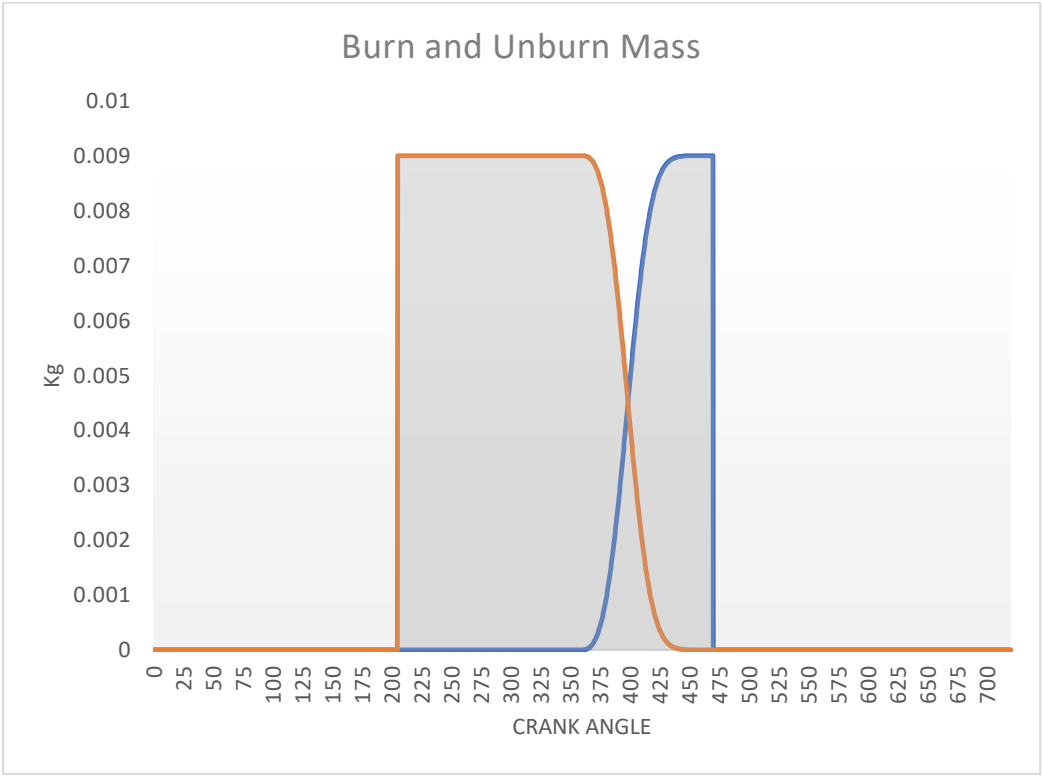

Figure IV.2.5.1 Burn and Unburn Mass

After that, the unburn temperature can be calculated by using equation (2.13). The step after this is calculating the burned temperature. Equation (2.14) can be used to determine the burned temperature, although the function B and A^* have to be determined first by using equation (2.17) and (2.18). To calculate the mix temperature can be seen from the equation down below.

$$Tmix = \frac{(c_{vburn}\, x\, m_{burn}\, x\, T_{burn})+(c_{vunburn}\, x\, m_{unburn}\, x\, T_{unburn})}{(c_{vburn}\, x\, m_{burn})+(c_{vunburn}\, x\, m_{unburn})} \quad \ldots (4.1)$$

The resulted temperature is illustrated by the figure below.

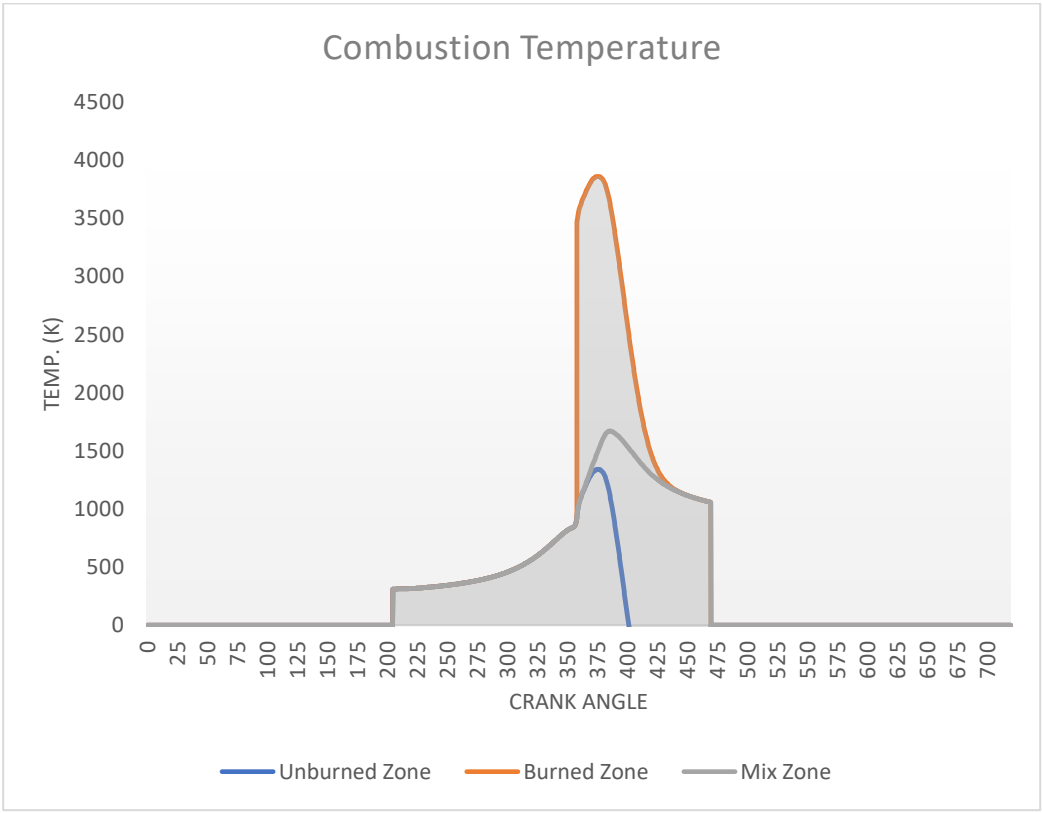

Figure IV.2.5.2 T burn, T unburn and T mix

The graph shows an overview of combustion temperature from the unburned zone, burned zone and mix zone. All of the zone has the same trendline, where the temperature starts rising prior the TDC and gradually decrease for the power stroke. The blue graph represents the unburned temperature, where it starts rising at 205° (intake valve closed) due to the effect of compression stroke. The temperature starts rising until it reached the 360° CA (TDC) and will gradually decreased due to the power stroke. Furthermore, the burned temperature which represent by the orange graph has the highest temperature around 3862 K at 376,75° and at the same time the unburned temperature also reached its highest temperature with 1341 K. After that, the outlet valve will open at 470° CA and the burned temperature have a value of 1060 K and the unburned temperature cannot be determined because the real value only last until 400° CA. In addition, the green graph represents the mix zoned temperature, where it is determined by using the equation (4.1). The mixed zone shows the combination of burned and unburned temperature inside the combustion chamber.

IV.2.6 Internal Energy

Basically, the internal energy is using the First Law of Thermodynamics as its idea. Where the energy cannot be destroyed but only can transform into different form. To calculate the internal energy, there are several parameters that have to be determined first. For example, the heat transfer (Q_w), heat release (Q_f) and mechanical work (W). The heat transfer can be calculated by using equation (2.21). Although the A_{liner} had to be obtained first by using equation (2.22).

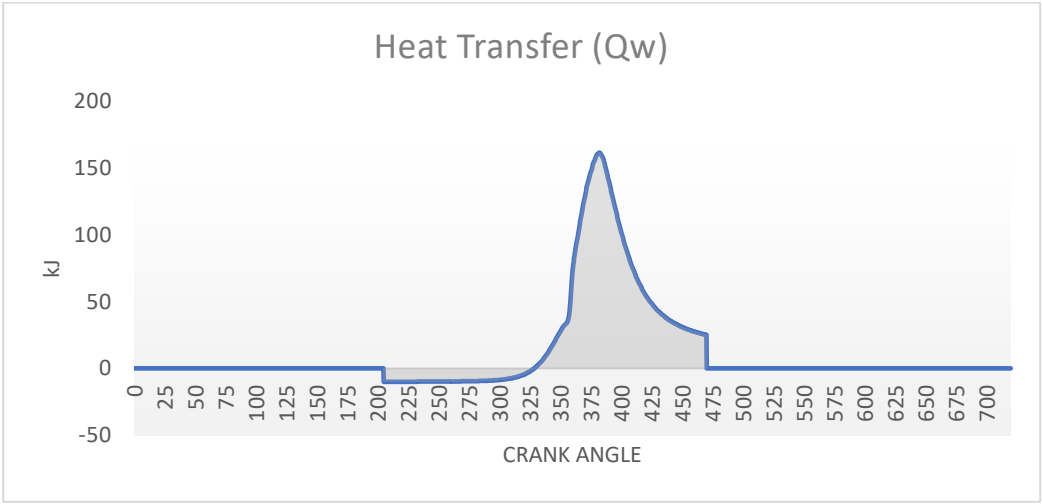

Figure IV.2.6.1 Heat Transfer

From graph above can be concluded that the bigger the surface area and heat transfer coefficient, the bigger the Q_w will be. While the heat release can be calculated by using equation (2.25), (2.26), (2.27).

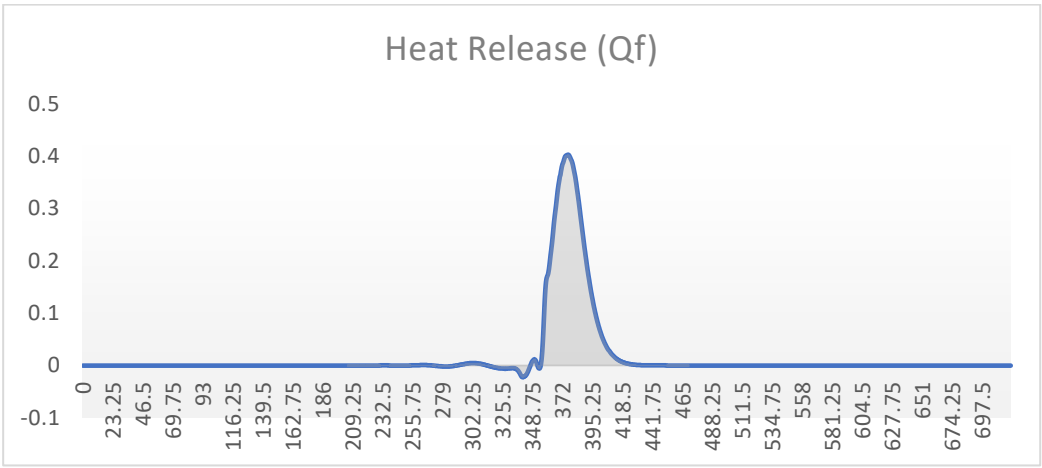

Figure IV.2.6.2 Heat Release

The heat release began to rise when the crank angle reached 352.25° and decrease rapidly until 361.25°. This condition is called premixed phase. After that, the mixed phase begin and the heat release starts to rise again until it reached its peak at 374° and gradually decrease to 0 KJ at 420.75°. The last parameter that need to be determined is mechanical work. The mechanical work can be determined by using equation (2.13).

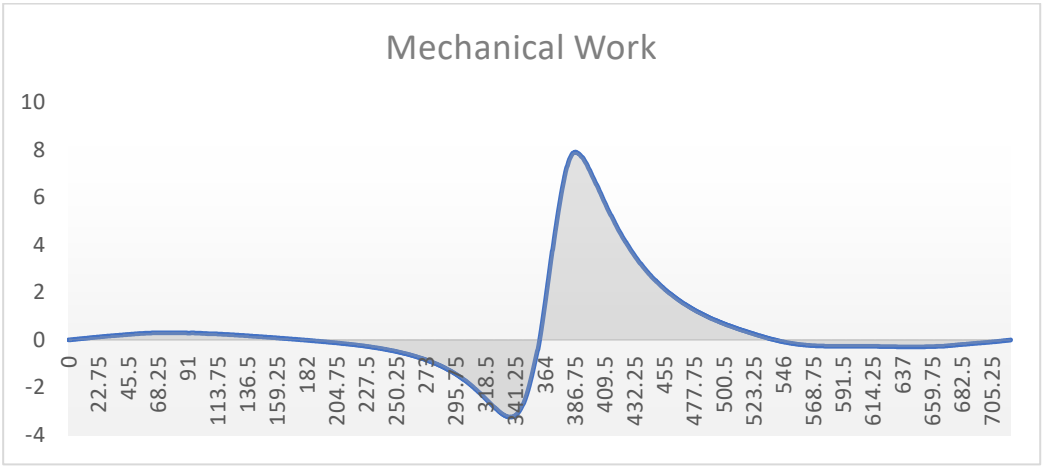

Figure IV.2.6.3 Mechanical Work

From the graph above can be seen that the mechanical work produces a negative and positive work. The negative result means that the piston produce a work in order to move the piston from BDC to TDC. After the piston reached the TDC, the piston will receive work from the combustion pressure. Therefore, when the piston moved from TDC to BDC the mechanical work has positive results.

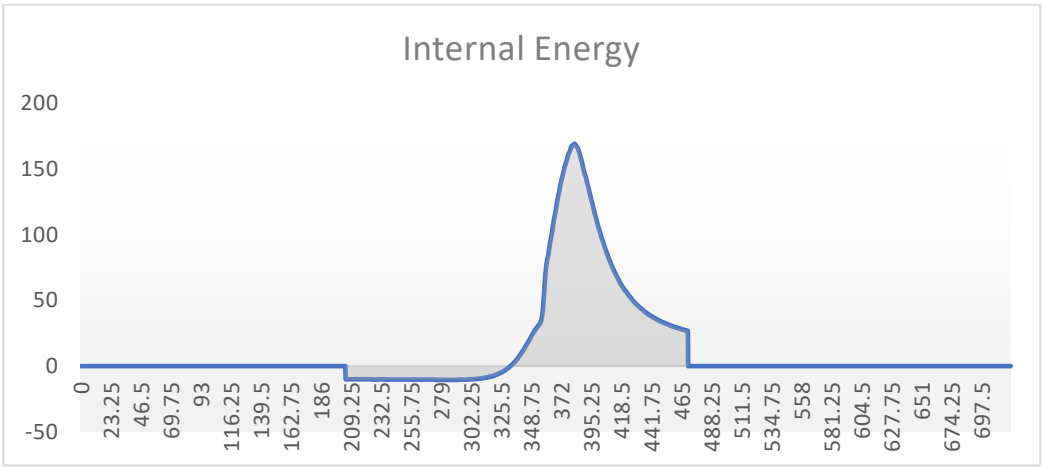

Figure IV.2.6.4 Internal Energy

The internal energy can be determined by using equation (2.20). The biggest parameter that affect the internal energy is the heat energy. And that explain why the trendline are almost the same as the heat transfer (Q_w).

IV.2.7 Secondary Chamber

IV.2.7.1 Basic Idea

The idea of this secondary chamber is basically the same as the Volkswagen invention. However, this idea is designed for the CI engine and also the piston inside the secondary chamber will be drive by a spring.

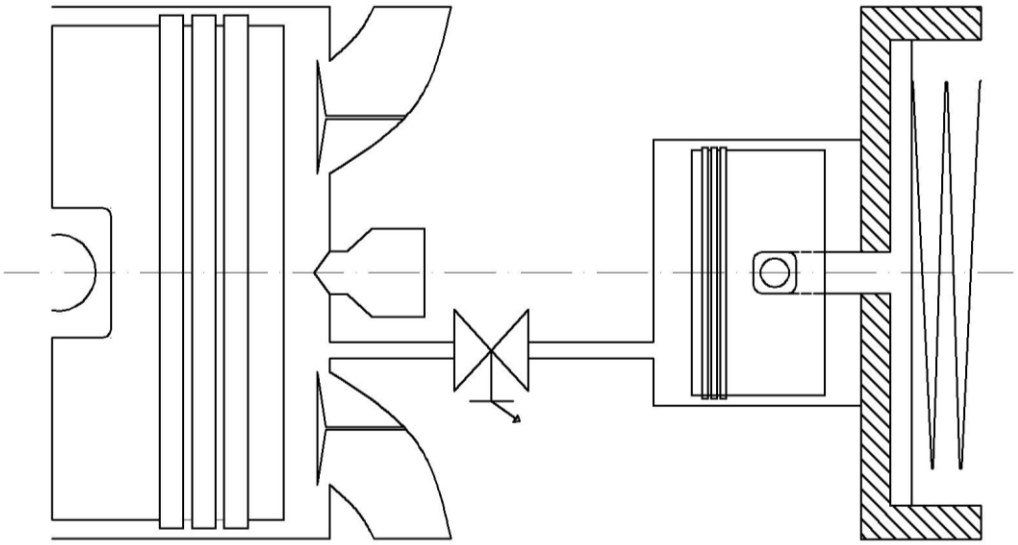

Figure IV.2.7.1.1 Secondary Chamber

The spring will deflect if the combustion pressure has exceeded the spring activation pressure, which allow the spring to deflect and created a bigger volume to store the energy from the combustion into the secondary chamber. When the pressure starts to decrease, the spring will start to expand and release the gas energy that was stored before. Hence, the purpose of this invention is to reduce the combustion temperature and keep the combustion pressure constant.

IV.2.7.2 Spring Parameter

There are a few parameters that have to be determined prior designing a spring such as the minimum and maximum pressure of the load. The minimum load will be taken from the compression pressure when the combustion

happened, which means that if the cylinder pressure has reached the targeted value. The spring will start to deflect and expanding the energy storage volume. The maximum pressure will be taken from the peak cylinder pressure.

Table IV.2.7.2.1 Minimum and Maximum Working Load

	P (bar)
Maximum Pressure	109.6
Activation Pressure	70
ΔP	39.6

After that, the spring will be calculated and designed as the working load requirement. To calculate the deflection (4.2), the spring constant must be determined first by using equation (2.33).

$$\delta = \frac{\Delta F}{k} \dots (4.2)$$

The detail specification of the spring will be described in the next chapter. The deflection of the spring will be used as the stroke of the secondary chamber. There will be two spring that designed to handle each of their cylinder liner bore sizes and a stopper to adjust the spring maximum deflection

Table IV.2.7.2.1 Minimum and Maximum Working Load

		100 mm	120 mm	units
Spring Constant	k	953.78	1898.28	N/mm
Deflection	δ	10	5	mm

After all of the necessary spring parameter has been determined. The step after this is to design the energy storage volume.

IV.2.7.3 Energy Storage Volume

The amount of energy and gas volume stored are depending on the volume of energy storage. So, determining the right piston bore and also the TDC volume of the chamber are very critical. In this graph below the value of piston bore will be simulated into two different sizes 100 mm and 120 mm with each of it have its own spring that has been optimized. The equation to determine the pressure is by using the Boyle's law.

$$P1.V1 = P2.V2 \dots (4.3)$$

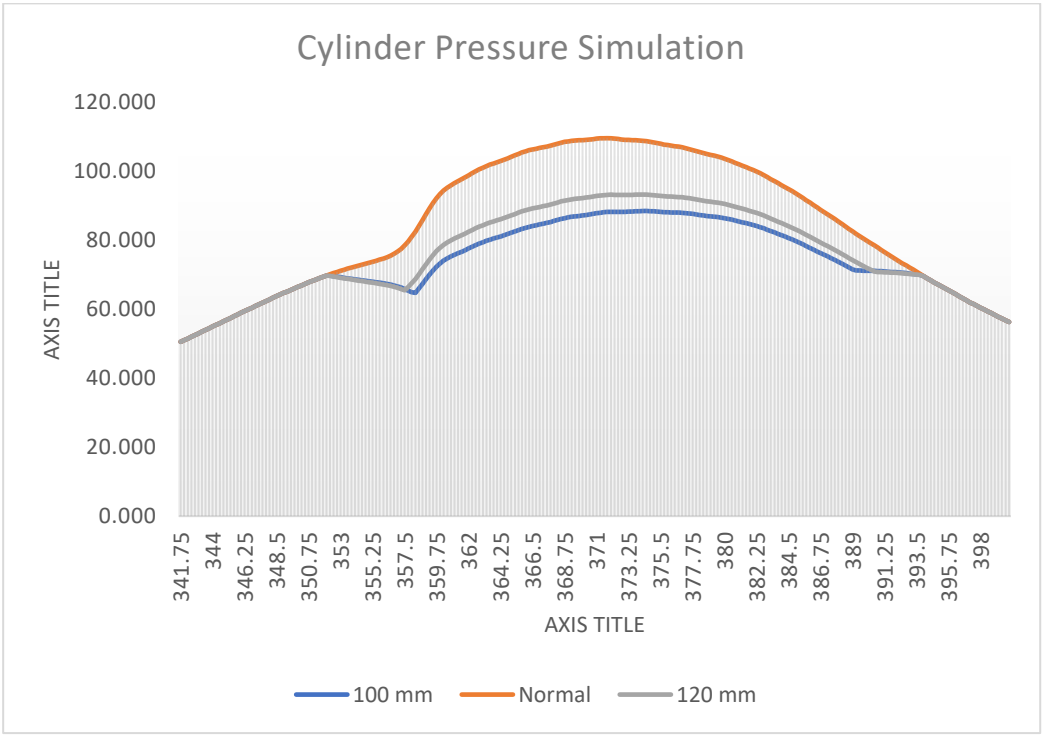

Figure IV.2.7.3.1 Cylinder Pressure Simulation

By using a simple pressure volume relationship, the result of the cylinder pressure is assumed without any heat energy interchange. Therefore, the best piston bore size is the one who can keep the combustion pressure constant. After going several optimizations, there will be two piston that will be installed into the secondary chamber with one of them replacing one another and have their own cylinder liner sizes.

Table IV.2.7.3.1 Secondary Chamber Specification

Secondary Chamber Specification				
Bore	=	120	100	mm
		0.12	0.10	m
Stroke	=	5	10	mm
		0.0322	0.236	m
Area Piston	=	0.001131	0.00785	m2
Area Chamber	=	0.00226195	0.0157	m2
Activation Pressure	=	70	70	Bar
Activation Force	=	79168.1	54977.9	N

From the table above, the activation pressure is obtained from the spring minimum working load, as the movement of the piston is controlled by the spring.

IV.2.7.4 Secondary Chamber Energy

The energy inside the secondary chamber will be calculated using the First Thermodynamic Law. Where the internal energy interchange will happen if the spring have start deflecting.

$$\Delta U\ Energy\ Storage = \Delta Uconventional - \Delta Unew\ pressure \ldots (4.4)$$

$$\frac{dU}{d\varphi} = \left(\frac{dQ1}{d\varphi} - \frac{dW1}{d\varphi}\right) - \left(\frac{dQ2}{d\varphi} - \frac{dW2}{d\varphi}\right) \ldots (4.5)$$

So, according to the equation (4.4) there are two parameters that has to be determined, the spring work and the secondary chamber heat energy. The deflection has a major influence to the spring work. As the spring work equation is.

$$W_{spring} = \frac{k\ x\ \delta^2}{2} \ldots (4.6)$$

Therefore, the spring will have different value of work depending on its deflection. Since, the spring constant/rate is constant. In this calculation the 100 mm bore sizes will be taken as the example. The graph down below illustrates the spring deflection based on force.

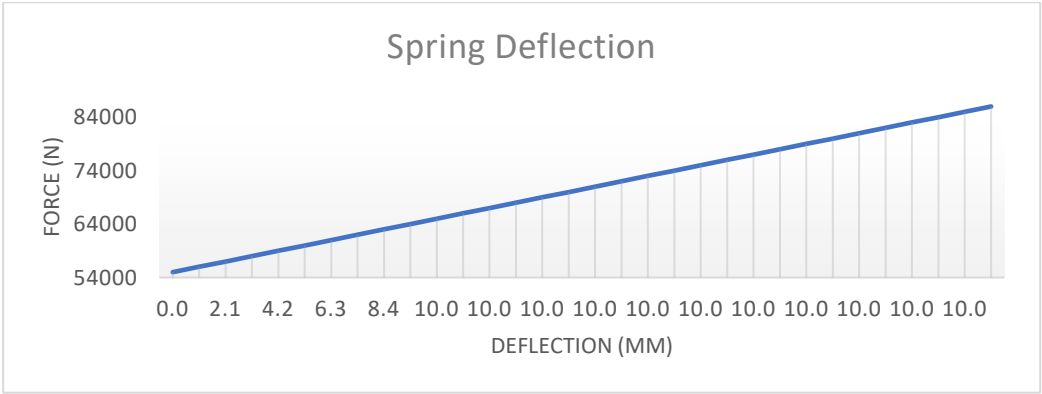

Figure IV.2.7.4.1 Spring Deflection

On the other hand, there is another way to calculate the spring work by calculating the area below the graph. Hence, each deflection will have a different

value of work. The graph down below illustrates the spring work over different value of deflection.

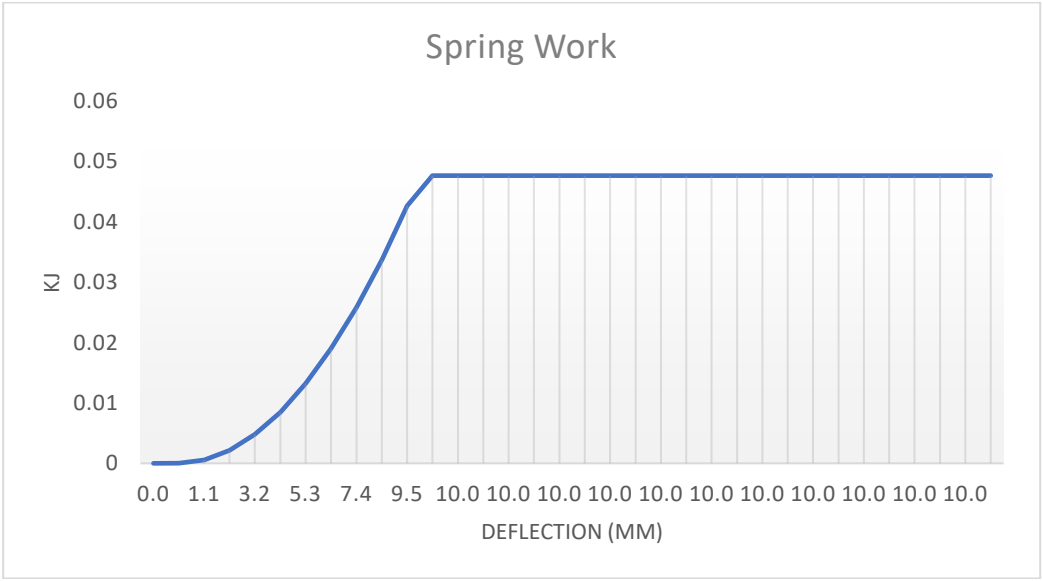

Figure IV.2.7.4.2 Spring Work over Deflection

The next step is to simulate the spring work based on the crank angle. Each of crank angles has its own cylinder pressure value. Therefore, when the spring starts to deflect, it will store the work energy from the combustion and will release it if the pressure has start to decrease. Since the stopper is set for a 10 mm deflection, hence deflection beyond that value is impossible.

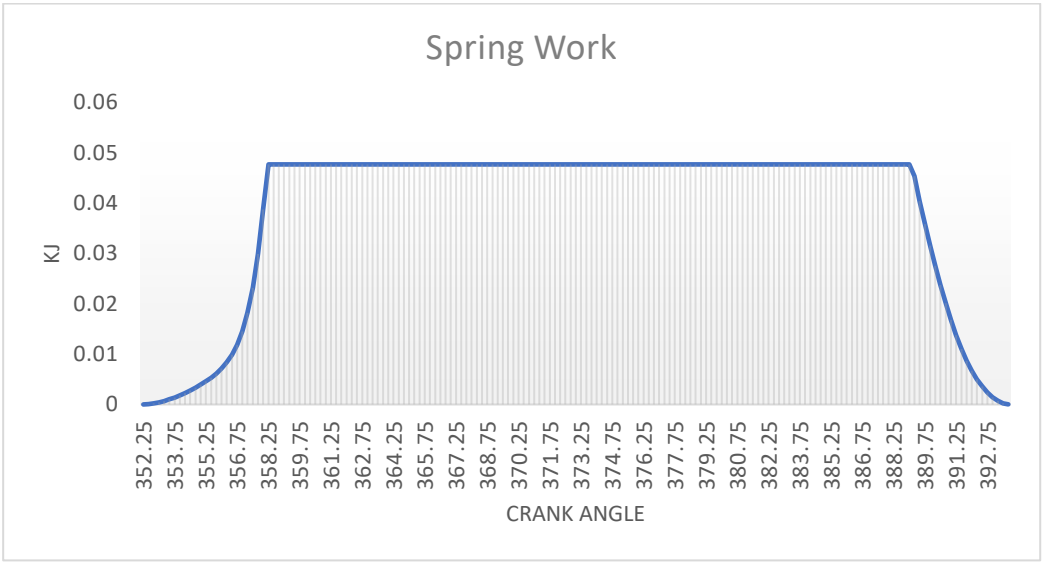

Figure IV.2.7.4.3 Spring Work over Crank Angle

From the graph can be seen that the spring started to deflect at 352.25° CA due to the cylinder pressure have exceeded the spring activation pressure. Then at 371.75°, it is the point where the spring have the highest amount of force as it's correlated with the cylinder pressure. And at 393.5°, the spring has released its last work energy since the cylinder pressure has decreased lower than the activation pressure. After that, equation (4.4) will be used to calculate how much internal energy can the secondary chamber stored.

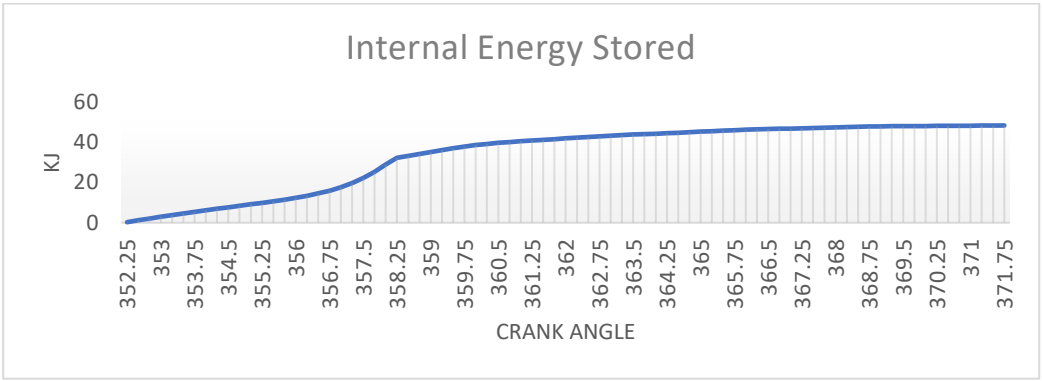

Figure IV.2.7.4.4 Energy Stored

From the graph can be seen that at 352.25° C.A, the internal energy stored started to rise gradually due to the cylinder pressure exceeded the activation pressure. The value keeps rising until 371.75° C.A, where the amount of the internal energy stored reached its maximum point with 91.9 kJ. After that, the internal energy stored will be released into the combustion chamber.

IV.2.7.5 New Cylinder Pressure

Due to the installation of the secondary chamber into the engine, there is a changing to the cylinder pressure. As the secondary chamber can stored the energy and release it later, there will be a new pressure calculation that can be seen in the equation below.

$$P = \frac{2\ x\ \Delta U_{secondary\ chamber}}{\frac{\pi}{4} x\ bore^2\ x\ \delta} \quad \ldots (4.7)$$

The new cylinder pressure will have a reduced peak pressure which resulted from the secondary chamber. The graph down below illustrates the comparison between the old cylinder pressure and the new cylinder pressure.

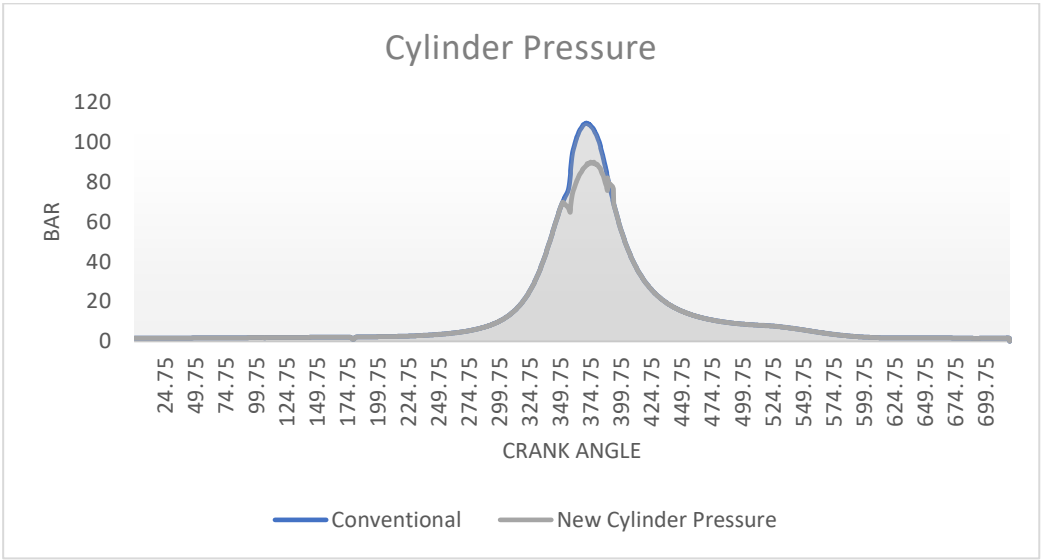

Figure IV.2.7.5.1 Cylinder Pressure Comparison

From the graph can be seen that at 352.25° CA, the cylinder pressure began to have a constant value due to the opening of secondary chamber valve until it reached 371.75° CA. Where the internal energy that has been stored will be released into the main combustion chamber until 393.75° C.A.

IV.2.8 Burn and Unburn Temperature Comparison

As a result of reducing the peak cylinder pressure, the burn and unburn fraction temperature value will be affected as according to equation (2.8) and (2.10) cylinder pressure is one of the parameters that have an influence to the temperature. The purpose of installing the secondary chamber is to reduce the temperature of combustion that will cause the NOx formation to decrease. The graph below illustrates the comparison between the conventional burned temperature and the modified secondary chamber burn temperature.

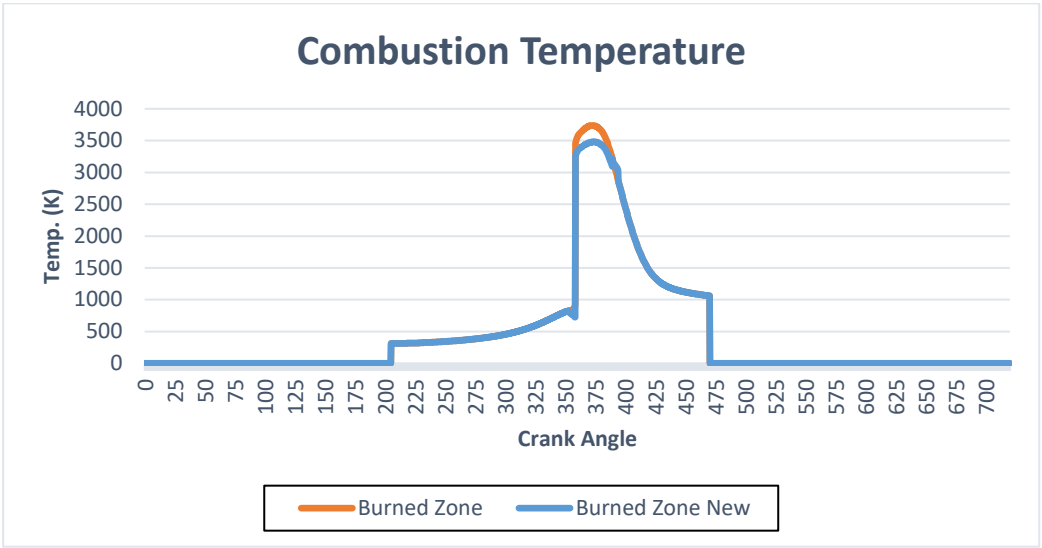

Figure IV.2.8.1 Burn Temperature Comparison

From the graph above can be seen that there is slight difference in the peak temperature, where at 376.75° CA the conventional burned had the highest temperature with 3853 K. While the modified burned temperature had its highest temperature at 377,75° with 3616 K. In conclusion, the modified burned peak temperature has a smaller value around 6.15% from the conventional temperature.

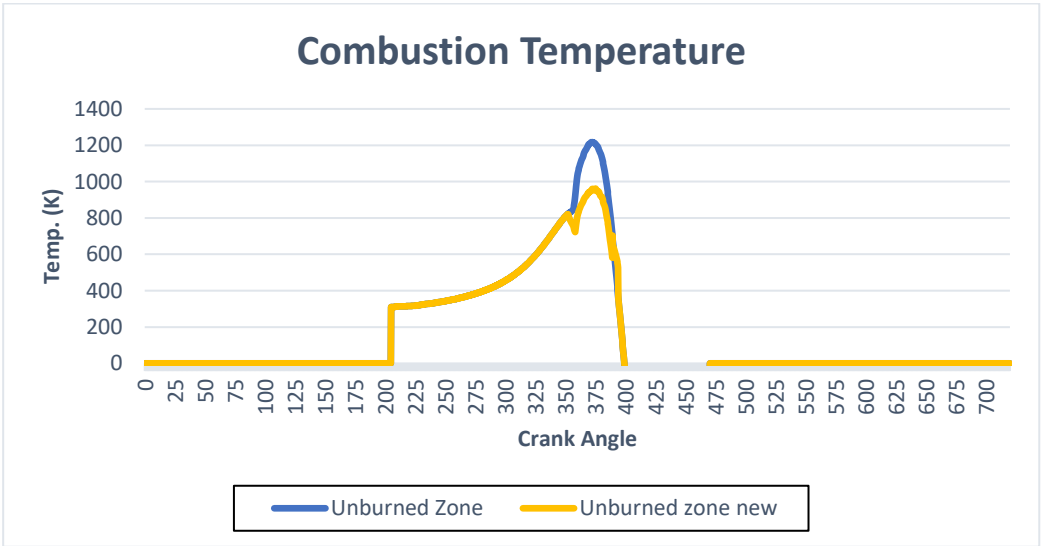

Figure IV.2.8.2 Unburn Temperature Comparison

The graph above illustrates the conventional and modified unburned temperature. There is a significant difference on the peak temperature, where the

conventional unburned temperature had a value of 1332 K at 376,75° CA and the modified unburned temperature had 1094,5 K at 377,75° CA. The difference between them is 17,8%, that is a big difference and shows that the secondary chamber proves can reduce the combustion temperature effectively.

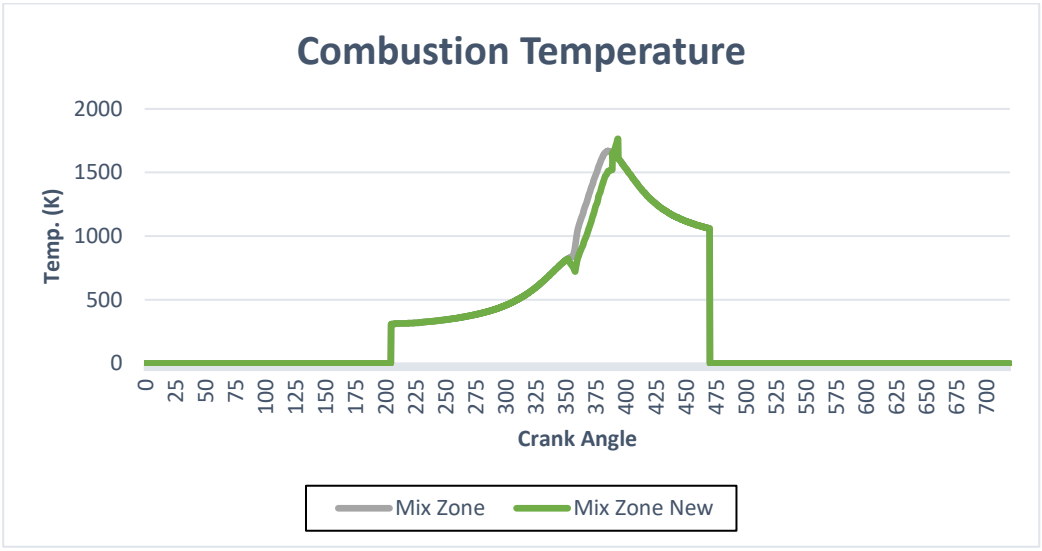

Figure IV.2.8.3 Mix Temperature Comparison

The graph above shows a comparison between conventional mix temperature and modified mix temperature. The maximum conventional mix temperature occurred at 385.5° C.A with 1663,8 K, while the maximum modified temperature happened at 394° C.A with 1766 K. There is big difference at 352,5° – 371,75° C.A where the modified mix temperature reached its peak temperature later due to the internal energy stored in the secondary chamber. In addition, from 371,75° – 393,75° C.A the internal energy that has been stored started to be released and causing the new modified mix temperature to have higher value than the conventional temperature.

IV.3 Design of The Energy Storage

There are several parameters that needed to be analyze prior designing the secondary chamber. The main priority is the material since the chamber will be working in the high thermal load environment. Therefore, thermal expansion of the material and also the strength have to be cautiously calculated.

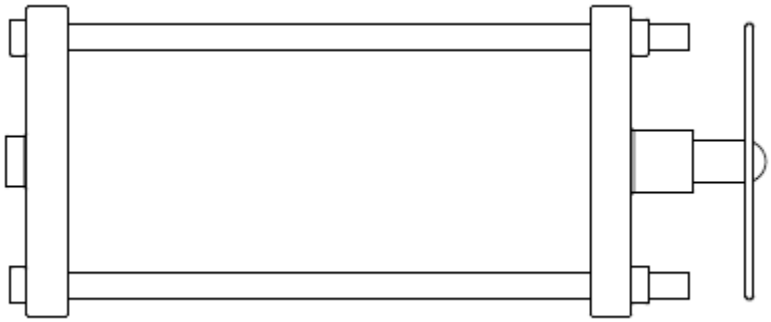

Figure IV.3.1 Energy Storage Design

There are nine parts to assemble the energy storage

1. Top
2. Bottom
3. Liner 100 mm
4. Liner 120 mm
5. Piston 100 mm
6. Piston 120 mm
7. Spring seater 100 mm
8. Spring seater 120 mm
9. Spring compressor
10. Stopper

There will be two materials that will be used to form the energy storage. Ceramic and Aluminum Alloy. All of the liner and piston will use a ceramic material that has properties as the following table.

Table IV.3.1 Ceramic Properties

Source: Ferro Ceramic

Ceramic Properties			
Chemical Formula	=	Si_3N_4	
Density	=	3.31	g/cm3
Compressive Strength	=	689 - 2760	MPa
Tensile Strength	=	360 - 434	MPa
Flexural Strength (MOR)	=	679 - 896	MPa
Max. Temperature load	=	1500	°C
Thermal Shock Resistance (ΔT)	=	750	°C
Coefficient of Linear Thermal Expansion	=	3.4	*10^-6/°C
Modulus Young (E)	=	317	GPa

The pistons will have undergone through a thermal analysis simulation using a software called *Ansys*. The displacement expansion is shown in figure IV.3.2 and IV.3.3. While the table below shows the specification of the Piston 1 and 2.

Table IV.3.2 Piston Specification

		Piston 1	Piston 2	Units
Diameter	=	100	120	mm
Area	=	0.007853982	0.011309734	m2
Temperature Min	=	25	25	C
Temperature Max	=	500	500	C

The picture below illustrates the displacement expansion due to thermal load. The piston was simulated in the high thermal load environment (25°C – 500°C). The red to blue color indicator indicates how much the radius changes from the center of the piston through the outer part.

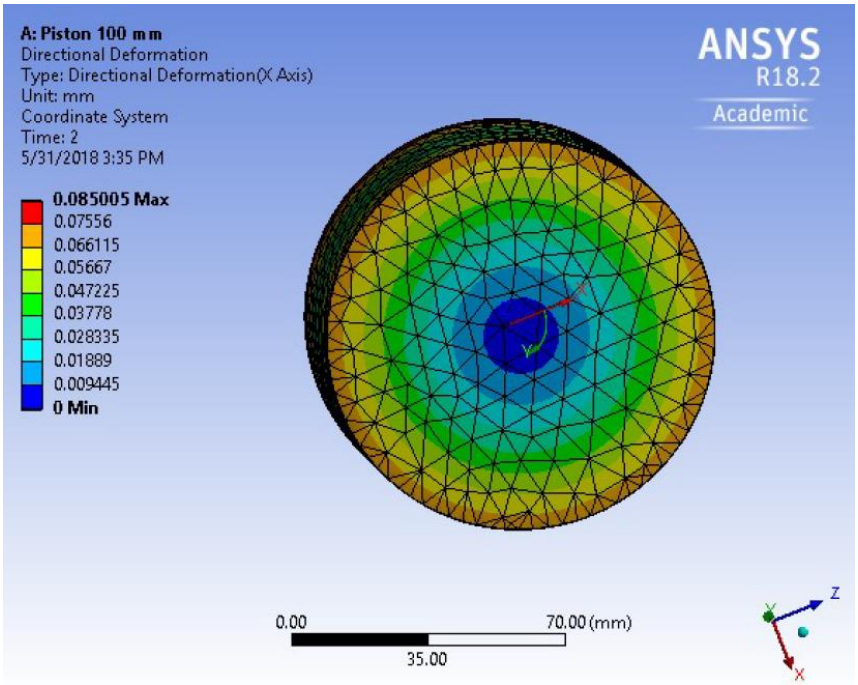

Figure IV.3.2 Piston 100 mm

The picture above is the 100 mm Piston. Where it can be seen that the outer section has the most expansion than any other area, which caused by convection. In addition, the maximum thermal expansion at the piston crown (Δr)

is 0.076 mm. That variable is very important to design the gap between the piston and the liner.

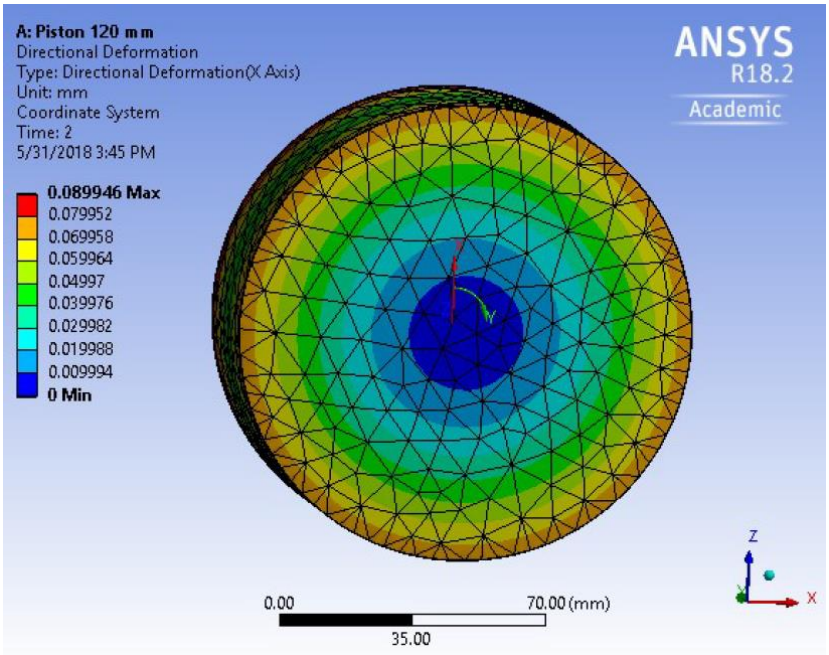

Figure IV.3.3 Piston 120 mm

While, the figure above illustrates the 120 mm Piston. The maximum thermal expansion occurred in the same area as the previous one. However, the value is even bigger due to bigger diameter with 0.080 mm. After the pistons have been simulated, the next step is to simulate the cylinder liner. The table down below shows the specification both of the cylinder liners.

Table IV.3.3 Liner Specification

		Liner 1	Liner 2	Units
Maximum Pressure	=	109	109	bar
Diameter	=	100	120	mm
Thickness	=	7	7	mm
Temperature Min	=	25	25	C
Temperature Max	=	500	500	C
Length	=	328.20	328.20	mm

The liner will be simulated in extreme thermal environment with the temperature range from 25°C to 500°C. For the liners case it is more complex than the piston since both of the cylinder liner ends were supported by the top and bottom part of the secondary chamber.

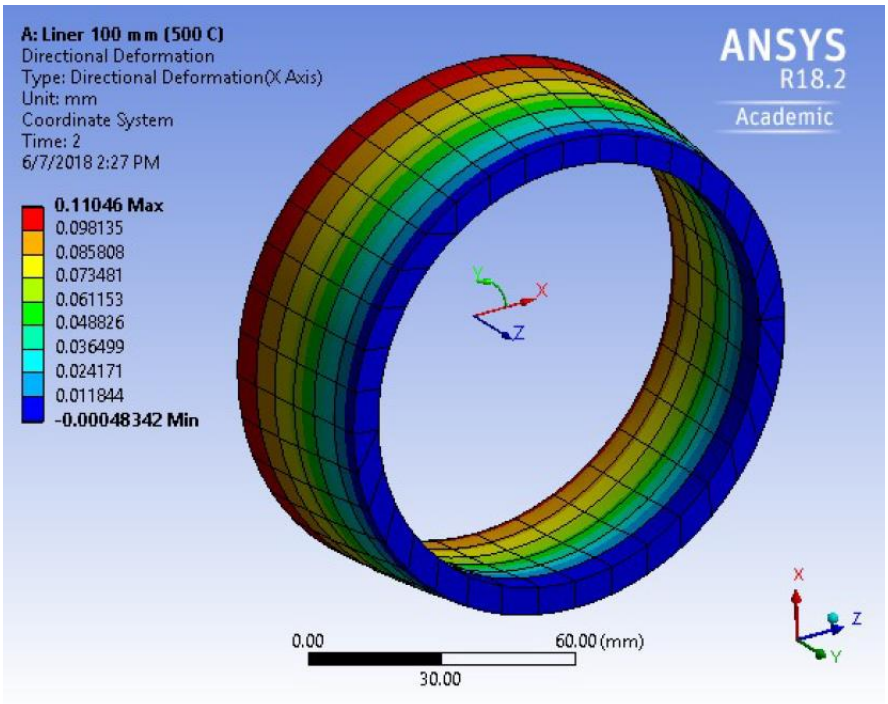

Figure IV.3.4 Liner 100 mm

The picture above shows the thermal expansion of the 100 mm liner. According to the picture above the end part of the liner suffer a decreased of displacement. And in the middle area is the area where the thermal expansion has its bigger value with 0.13 mm. However, it is also important to consider the thermal expansion in other area. Several important information will be showed down below.

- Max. thermal expansion = 0.11 mm
- Thermal expansion where the piston will be positioned = 0.048 mm

The equation down below shows how to calculate the liner gap.

$$Minimum\ Gap = \Delta \mathrm{r}\max piston - \ \Delta r\ liner\ (piston\ positioned) \ldots (4.8)$$

Subs.

$$100\ mm\ Liner\ Gap = 0.076\ \mathrm{mm} - 0.048$$
$$100\ mm\ Liner\ Gap = 0.028\ \mathrm{mm}$$
$$100\ mm\ Liner\ Gap = 0.04\ \mathrm{mm}$$

The gap between 100 mm liner and 100 mm piston is 0.028 mm. However, to simplify the manufacturing process and for safety reason 0.04 mm will be taken as the liner gap.

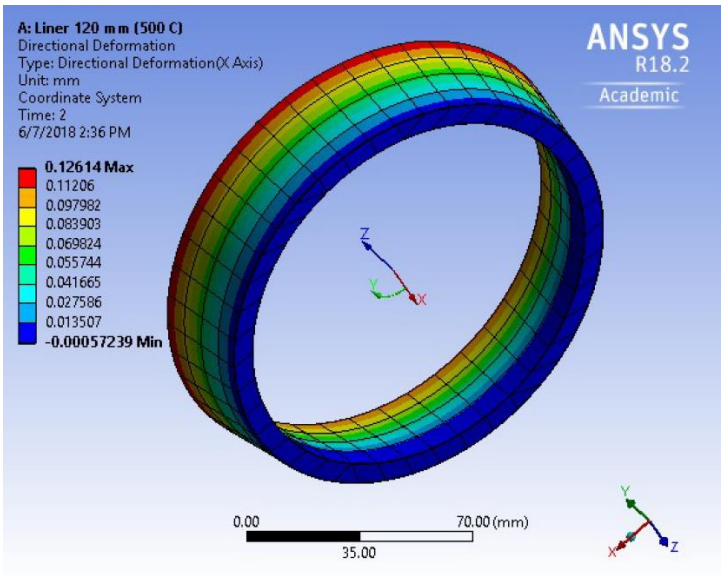

Figure IV.3.5 Liner 120 mm

The figure above illustrates the 120 mm liner. From the picture can be seen that the end part of the liner also suffers a decreased of displacement. And the middle has the biggest expansion with 0.145 mm.

- Max thermal expansion = 0.14 mm
- Thermal expansion where the piston will be positioned = 0.055 mm

The liner gap can be calculated using equation (4.8).

Subs.

$$120\ mm\ Liner\ Gap = 0.80\ \text{mm} - 0.55$$
$$120\ mm\ Liner\ Gap = 0.025\ \text{mm}$$
$$120\ mm\ Liner\ Gap = 0.04\text{mm}$$

The gap between 120 mm liner and 120 mm piston is 0.25 mm, but for safety reason and to simplify the manufacturing process 0.04 mm will be taken as the gap. The last part that needs to be simulated is bottom part of the secondary chamber, where the material that been used is an aluminum alloy.

Table IV.3.4 Aluminum Alloy Properties

Aluminum Alloy Properties			
Modulus Young	=	68.3	GPa
Density	=	2.6898	g/cm^3
Thermal Expansion Coefficient	=	0.0000235	/°C
Tensile Strength	=	690	MPa
Maximum Temperature Load	=	700	°C

Since the bottom and the top part of the secondary chamber has the same dimension, hence it is possible to only simulate one of the parts because it has the same expansion characteristics. The table down below shows the specification of the bottom part of the secondary chamber.

Table IV.3.5 Bottom Specification

		Top	Units
Diameter	=	100.12	mm
Thickness	=	30	mm
Temperature Max	=	250	C
Temperature Min	=	25	C
Length	=	150 x 150	mm

The areas that are very important for the liner design are the area where the cylinder liner will be seated. The picture down below illustrates the bottom part of the secondary chamber that has been simulated in a high thermal load environment (25°C – 250°C) since the inlet of the bottom part of the chamber will be insulated tha maximum temperature will be assume 250°C.

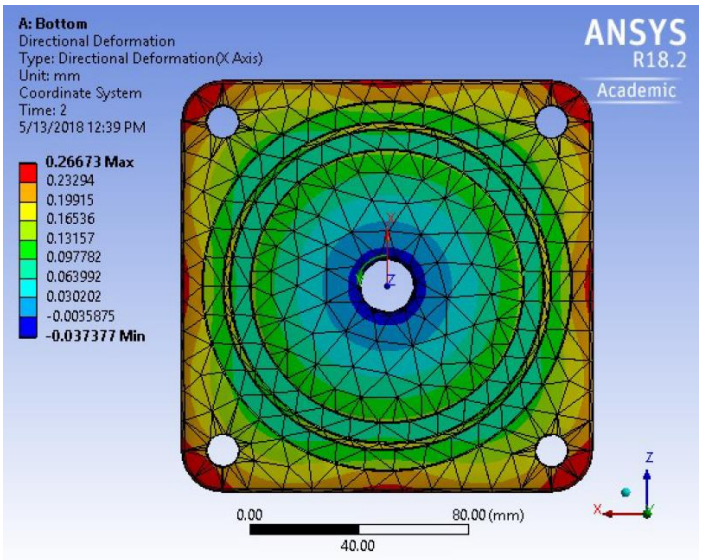

Figure IV.3.6 Bottom Part of The Secondary Chamber

From the picture above can be taken that the thermal expansion that occurred in the cylinder liner seat is 0.14 mm. Which means that the gap between the liner and the bottom and top parts of the secondary chamber is 0.14 mm. The complete picture of the secondary chamber will be attached in the appendix.

IV.4 Spring Design

There are two steps for designing a spring, the non-linear optimization and geometry optimization. First of all, non-linear optimization is a process to optimize the spring activation pressure by converting the pressure load into force.

Table IV.4.1 Non-Linear Optimization

	P (bar)	Spring 1 (N)	Spring 2 (N)
Maximum Pressure – Force	109.6	86079.64	123954.7
Activation Pressure – Force	70	54978	79168
ΔF		31101.77	44786.54

The force of the springs above were divided by the piston bore area which is why there will be two spring design that each of them were optimized for each of the bore sizes.

Table IV.4.2 Piston Area

	Piston 1	Piston 2
Bore	100 mm	120 mm
Area	0.00785 m^2	0.01131 m^2

The step after this is the geometry optimization, where the spring will be designed not only able to withdrawn the pressure but also the amount of its deflection. Since both of the springs are working in the same high thermal load environment, hence both of it are using the same material.

Table IV.4.3 Spring Material

Chrome-vanadium alloy steel wire JIS SUP 10			
Modulus of elasticity at operational temperature	**G**	78500	MPa
Density	**ρ**	7850	kg/m3
Fatigue strength by finite life	**τf**	470	MPa
Ultimate tensile strength	**τe**	1350	MPa

The material is able to work up to 250°C thermal load, therefore chrome-vanadium alloy is the right material for the spring. After the material has been selected, the next step is to design the spring using equation (2.29), (2.30) …. (2.44). From the calculation can be taken the geometry of the spring design.

Table IV.4.4 Spring Geometry Design

Compression Spring		**Spring 1**	**Spring 2**
Number of active coils	n	5	5
Inactive coil	n'	2	2
Coil End	Squared Ground End		
Direction of coil winding	Right		
Spring constant [N/mm]	k	953.775	1898.28
Spring weight [kg]	m	2.686	5.571
Outer spring diameter [mm]	De	78	94
Inner spring diameter [mm]	Di	42	46
Free spring length [mm]	L0	280	280
Preloaded spring length [mm]	L1	222.358	238.295
Fully loaded spring length [mm]	L8	189.748	214.702
Theoretic spring limit length [mm]	L9	126	168
Minimum working loading [N]	F1	54977.9	79168.1
Maximum working loading [N]	F8	86079.6	123955
Theoretic spring limit loading [N]	F9	146881	212607
Spring material:			
Chrome-vanadium alloy steel wire JIS SUP 10			
Wire diameter [mm]	d	18	24

The table above describe the spring geometry design. Where it can be seen that both of the spring has the same free length. However, the deflection is varying since the wire diameter and the spring diameter are different. The characteristics of each spring can be described by spring deflection diagram, where the trendline is linear.

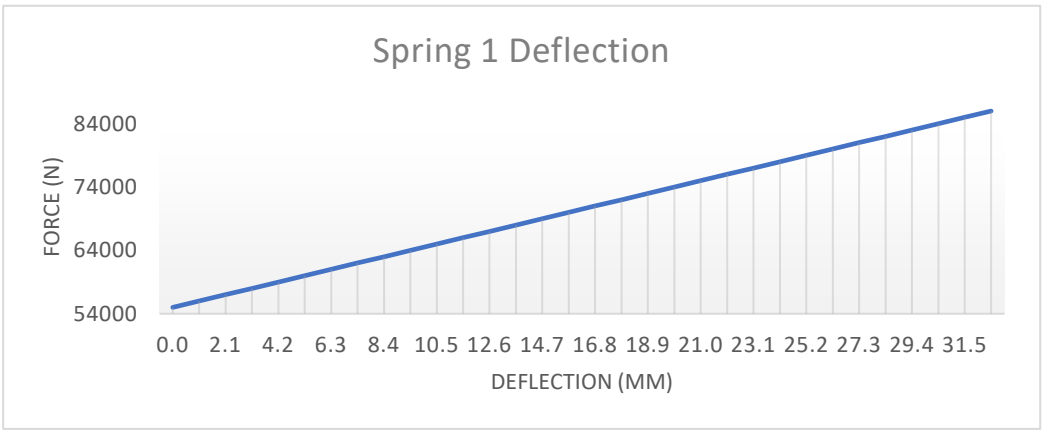

Figure IV.4.1 Spring 1 Deflection

According to the graph the higher the force, the higher the deflection would be. The maximum deflection for the spring one is 32,6 mm. With activation force around 55,000 N and 86,000 N to achieve the maximum deflection.

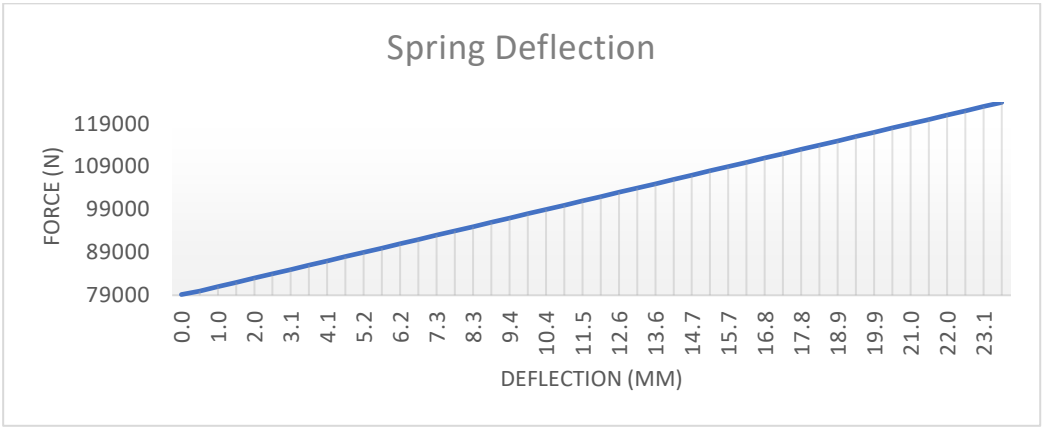

Figure IV.4.2 Spring 2 Deflection

From the graph above can be taken that the maximum deflection for the spring two is 23,6 mm. With activation force around 79,000 N and 119,000 N for maximum force.

IV.5 Pipeline Losses

The external chamber system requires a pipeline to connect its inlet with the indicator cock. The indicator cock is directly planted in the cylinder head to distribute the combustion gas into the external chamber. The figure down below illustrates the external chamber system.

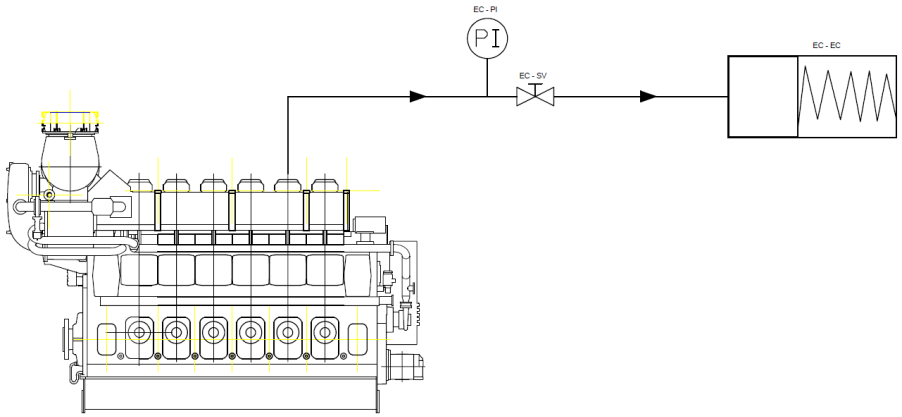

Figure IV.5.1 External Chamber System

From the picture can be seen that pressure indicator and solenoid valve are installed in the pipeline system. There are two losses that occurred inside the pipeline, the pressure loss and heat loss. The pressure loss can be divided into three losses, the major loss, minor loss and the static loss (Carello et al, 1998). Major loss in pipeline is caused by the friction between fluid and inner surface of the pipeline. The equation (4.9) until (4.12) explain how to calculate the major loss.

$$P_{major\ loss} = \lambda . \rho . \frac{v^2}{2} . \frac{L}{D} \text{ .... (4.9)}$$

Where λ is the friction factor that can be obtained by using equation (4.10).

$$\lambda = \frac{1}{\left(2 \log\left(0.5625 . Re^{\frac{7}{8}}\right) - 0.8\right)^2} \text{ ... (4.10)}$$

The Reynold number can be calculated using equation (4.11) with the gas viscosity (μ) obtained from equation (4.12).

$$Re = \frac{\rho . D}{\mu} . v \text{ ... (4.11)}$$

$$\mu = \left(1.84 - \left(\frac{300 - T}{300}\right)\right) . 10^{-5} \text{ ... (4.12)}$$

The specification of the pipe is explained in the table down below. With the pipe dimension were taken from the JIS specification.

Table IV.5.1 Pipe and Calculation Information

Pipe and Calculation Information			
Length	=	0.3	m
Diameter	=	0.025	cm
h (z2 – z1)	=	0.05	m
Material	=	Chromium Nickel	
Max. Temp	=	1000	°C
Gravity	=	9.8	m/s2
R	=	0.082	atm.L/mol.K
Density	=	0.08	Kg/m3

Since the spring activation pressure is 70 bar, therefore the solenoid valve will start to open at 352.25° C.A when the combustion pressure has exceeded the activation pressure. The losses calculation is started at 352.25° C.A as well.

Table IV.5.2 Major Loss Calculation Example

C.A	P [bar]	μ	Re	λ	P Maj loss [bar]
352.25	69.951	3.56571E-05	4904395902	5.69E-05	0.048

The table above shows that the major loss at crank angle 352.25 is only 0.048 bar. The major loss is very small due to the short length of the pipeline. Hence, the longer length of the pipeline, the bigger the major loss would be. While the static pressure occurred when there is a difference high between the suction and discharge point. Therefore, the height between those two points are consider very important in pipeline design. The equation (4.13) can be used to calculated the static pressure, with R stands for Gas constant (0.082 L.atm/K.mol).

$$P_2 = P_1 \,.\exp[\frac{-g\,.(z_2-z_1)}{R.To}] \ldots (4.13)$$

By using the above equation, the static pressure loss result can be described as the table below.

Table IV.5.3 Static Loss Calculation Example

C.A	P [bar]	T [K]	P Static loss [bar]
352.25	69.685	817.71	0.005

The table above shows that the static loss from the pipeline is 0.051 bar. From the equation can be taken that the bigger the (z2-z1) value the bigger the static loss would be. And since, it is exponential that means that a minor increase in the pipeline height can cause a major increase of static loss. On the other hand, the minor loss is cause by the fittings throughout the pipeline. The table down below describes the fittings throughout the pipeline.

Table IV.5.4 List of Fittings

List of Fittings		
	n	k
Globe Valve	1	7.8
T Joint	1	1
Elbow 90o	1	0.69
ΣK		9.49

To minor loss can be calculated by using the equation down below.

$$hf = k \cdot \frac{v^2}{2g} \ldots (4.14)$$

According to equation (4.14) the more fittings installed in the pipeline, the bigger the minor loss would be. The table down below shows the result of minor loss inside the pipeline.

Table IV.5.5 Minor Loss Calculation Example

C.A	P [bar]	Minor Loss [bar]
352.25	69.685	0.09 bar

After all of the pressure loss have been calculated, the pressure loss will be summed up. Hence, the total pressure loss will be the final resulted.

$$P_{total\ loss} = P_{major\ loss} + P_{minor\ loss} + P_{static\ loss} \ldots (4.15)$$

The total pressure loss is explained by the table down below.

Table IV.5.6 Minor Loss Calculation Example

C.A	Major Loss [bar]	Minor Loss [bar]	P Static loss [bar]	Total Loss[bar]
352.25	0.048	0.09	0.005	0.14

Figure down below shows the pressure drop that occurred at crank angle 352.25° – 393.5°. The pressure drop is almost constant. And there is no significance different between the normal pressure and (*normal-P loss*).

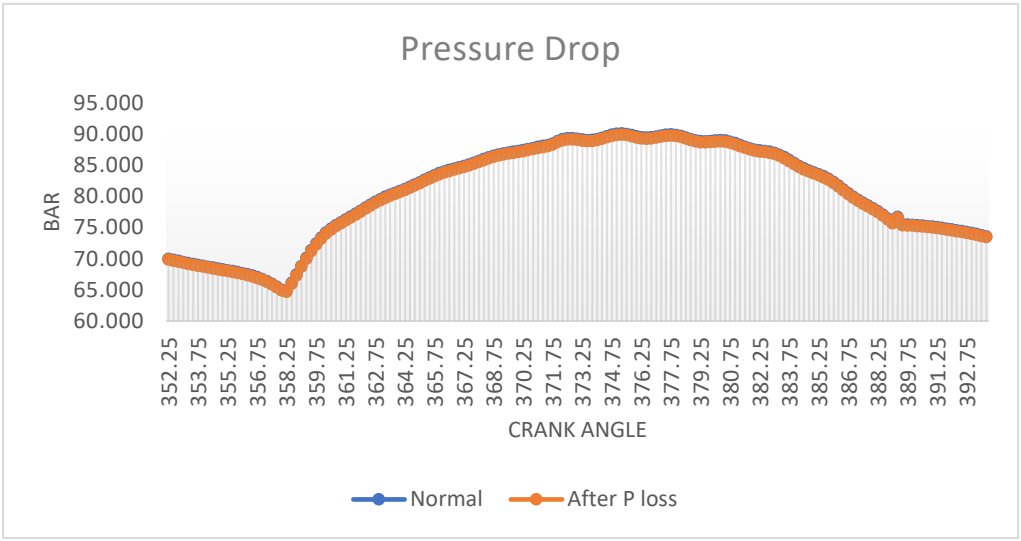

Figure IV.5.2 Pressure Drop per Crank Angle

Because the fluid is a high temperature gas, there will be heat losses that happened inside the pipeline via conduction and convection. In this calculation, there will be a comparison of heat losses between a pipeline with insulation and ordinary pipeline. Equation (2.43) explain about heat loss calculation in general that combine conduction and convection.

$$Q_{loss} = \frac{Ti-To}{Rt} . 2 . \pi . L \ldots (2.43)$$

$$Rt = \frac{1}{hi} + \frac{\ln\frac{R2}{R1}}{K\ pipe} + \frac{1}{ho} \ldots (2.44)$$

$$Rt = R_{fluid\ convection} + R_{conduction} + R_{ambient\ convection}$$

$$Rt = \frac{1}{h_i} + \frac{\ln\frac{R2}{R1}}{K_{pipe}} + \frac{1}{h_o} + \frac{\ln\frac{R3}{R2}}{K_{insulation}} \ldots (2.45)$$

$$Rtinsl. = R_{fluid\ convection} + R_{conduction} + R_{ambient\ convection} + R_{insulation\ conduction}$$

The *Rt* is the thermal resistance that depends on the thermal conductivity of the material and also the ambient environment. There will be two different thermal resistance where equation (2.44) is the equation for a pipeline without insulation and equation (2.45) is for insulated pipe.

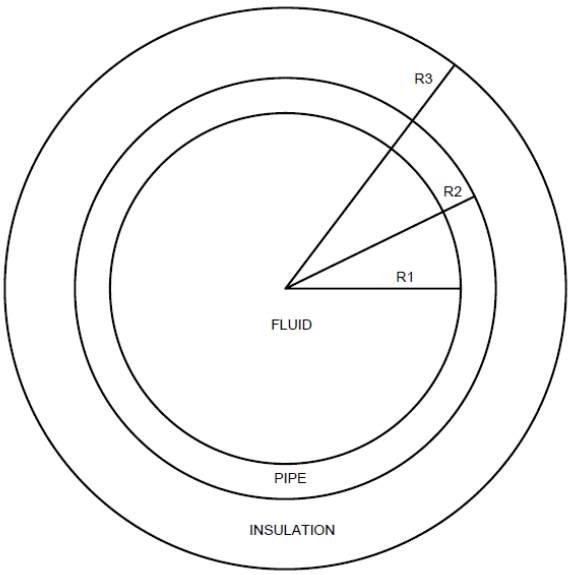

Figure IV.5.3 Pipeline Dimension

The figure above illustrates a cross section insulated pipe. The radius or thickness and material of the pipe is very important since it has an influence in the thermal resistance.

Table IV.5.7 Heat Loss Calculation Data

Data			
R1	=	0.0125	m
R2	=	0.015	m
R3	=	0.025	m
Stefan Boltzmann (σ)	=	5.67E-08	W/m2.k
Length	=	0.3	m
T Surface insulation	=	343	k
T Surface pipe	=	723	k

The table above shows the dimension of the pipeline system. The insulation surface temperature is assumed 343 K and the surface pipe temperature is 723 K with an assumption of 50 K temperature loss due to direct contact with the air. Practically, insulation is used to minimize the heat losses which occurred in the pipeline. Therefore, a comparison between them will give some essential information how effective the insulation would be.

Table IV.5.8 Pipe and Fluid Specification

Pipe (JIS Standard)			
Inner Diameter	=	0.025	m
Outer Diameter	=	0.03	m
K pipe	=	23	W/m.k
Material	=	Chromium Nickel	
Insulation			
Thickness	=	0.01	m
K insulation	=	0.1	W/m.k
Material	=	Calcium Silicate	
Emissivity	=	0.9	
Fluid Information			
Viscosity (μ)	=	0.000037	Pa.s
Heat Capacity (Cp)	=	1.099	kJ/kg.k
Thermal Conductivity (k)	=	0.0577	W/m.k
Density (ρ)	=	0.435	kg/m3
Heat Transfer Coefficient (hi)	=	56.8	W/m2.k
Coef. Vol. Expansion (β)	=	0.007322	m3/m3.K
Additional Information			
Gravity (g)	=	9.8	m/s2
K air	=	0.02735	W/m.K

The thermal resistance that can be calculated first is the fluid conduction and the pipe conduction.

$$R_{fluid\ convection} = \frac{1}{hi} \ \& \ R_{pipe\ conduction} = \frac{\ln\frac{R2}{R1}}{K\ pipe'}$$

$$R_{insulation\ conduction} = \frac{\ln\frac{R3}{R2}}{K\ insulation} \quad \text{.... (2.46)}$$

With h_i stands for the heat transfer coefficient of the fluid, K pipe is the thermal conductivity of the pipe and K insulation represents the thermal conductivity of the insulation. The table down below shows the result of the calculation using equation (2.46). As it has been shown from the equation, the result from the equation (2.46) is always constant, regardless the crank angle position.

Table IV.5.9 Thermal Resistance of the fluid and pipe

$R_{fluid\ convection}$	$R_{pipe\ conduction}$	$R_{insulation\ conduction}$
0.01760563	0.00792702	5.1082562

Meanwhile to calculate the thermal ambient resistance is a bit complex, since the ambient heat transfer coefficient (h_o) consist of $h_{radiation}$ and $h_{convection}$. The Nusselt number had to be used to calculate the $h_{convection}$. The equation (2.47) .... (2.54) shows how to calculate the enthalpy of the outside air.

$$h_o = h_{radiation} + h_{convection} \text{ .... (2.47)}$$

$$h_{radiation} = \sigma \,.\, \varepsilon \,.\, \frac{(Ti^4 - To^4)}{(Ti - To)} \text{ ... (2.48)}$$

$$h_{convection} = \frac{Nu\,.k_{ambient\ air}}{D_{max}} \text{ ... (2.49)}$$

Nusselt Number

$$Nu = \{0.6 + \frac{0.387\,.Ra^{\frac{1}{6}}}{\left[1+\left(\frac{0.559}{Pr}\right)^{\frac{9}{16}}\right]^{\frac{8}{27}}}\}^2 \text{ .... (2.50)}$$

Rayleigh Number

$$Ra = Gr.Pr \text{ ... (2.51)}$$

Prandtl Number

$$\Pr = \frac{\mu\,.Cp}{k} \text{ ... (2.52)}$$

Grashof Number

$$Gr = \frac{D^3.\rho^2.g.\Delta T.\beta}{\mu^2} \text{ .... (2.53)}$$

$$\beta = \frac{1}{\frac{(Ti+To)}{2}} \text{ .... (2.54)}$$

Where μ stands for the fluid or gas viscosity, β represents the coefficient of volume expansion of the fluid, k is the thermal conductivity of the fluid and Cp is the heat capacity. From the equation can be taken that the enthalpy of the ambient air is not constant. As the h_o is depend on the temperature $\frac{ho}{\partial T}$. Since the temperature is changing at every crank angle position, the h_o can be defined as follow $\frac{ho}{\partial \varphi}$.

Table IV.5.10 Outside Air Heat Transfer Coefficient

Pipe		**Ordinary**	**Insulated**
Crank Angle	=	352.25	
Prandtl Number	=	0.0007047	0.0007047
Pipe		**Ordinary**	**Insulated**
Grashof Number	=	2682.2792	17379.308
Rayleigh Number	=	1.8902863	12.247
Nusselt Number	=	0.36	0.36
$h_{convection}$	=	0.32820	0.19692
$h_{radiation}$	=	27.23084	47.001
h_o	=	27.55904	47.1983

From the table above can be taken that the insulated pipe has a bigger heat transfer coefficient for outside air than ordinary pipe with 47.2 W/m^2.k and 27.55 W/m^2.k respectively. This can occur because the insulated pipe temperature difference is way bigger than the ordinary one, since the insulation is keeping the heat energy inside the pipe. With all of the data have been known the total thermal resistance can be calculated as follow by using equation (2.44) and (2.45).

Table IV.5.10 Outside Air Heat Transfer Coefficient

Pipe		**Ordinary**	**Insulated**
Crank Angle	=	352.25	
$R_{fluid\ convection}$	=	0.0176056	
$R_{pipe\ conduction}$	=	0.00792702	
$R_{ambient\ convection}$	=	0.036286	0.02119
$R_{insulation\ conduction}$	=	-	5.1082562
R_{total}	=	0.0618184	5.1549

The insulated pipe has a bigger thermal resistance compared to ordinary pipe with 5.1549 and 0.0618184 respectively. This was caused by the insulation where the biggest thermal resistance is occurred. After calculating the total thermal resistance, all of the necessary data can be substitute into equation (2.43).

Subs.,

$$Q_{loss\ insulation\ (352.25)} = \frac{821.4 - 343}{5.1549} . 2 . \pi . 0.3$$
$$Q_{loss\ ordinary\ (352.25)} = \frac{821.4 - 723}{0.069143} . 2 . \pi . 0.3$$

Result,

$$Q_{loss\ insulation\ (352.25)} = 0.175\ kJ$$
$$Q_{loss\ ordinary\ (352.25)} = 3.0\ kJ$$

From the example above can concluded that the insulation method is very effective, since it can save more 94.1% of heat energy compared to ordinary one. Furthermore, insulation also provide more safety value to avoid human injury, as the fluid is very hot a direct contact with the skin can caused severed burned damage.

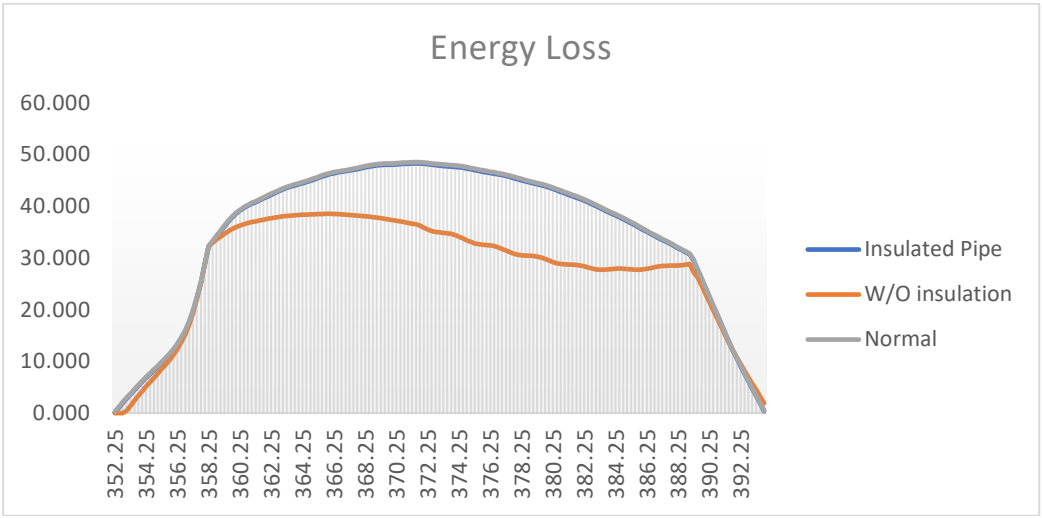

Figure IV.5.3 Heat Loss Comparison

From the graph can be seen that, there is a wide difference between the normal energy and the insulated pipe. Because, the heat loss that occurred inside the insulated pipe is small compared to w/o insulation. In conclusion, in this pipeline design an insulation made from asbestos will be installed throughout the length of the pipe.

CHAPTER V
CONCLUSION

From the thesis results, there will be five conclusion points that will answer the problem of the research, the answers are:

1. Based on the studies, the basic purposes of spring based connecting rod, C connecting rod and S connecting rod are to decrease the combustion pressure inside the combustion chamber by manipulating the cylinder volume or the compression pressure.
2. There are several parameters that are imperative to the calculation of the energy stored for example, compression pressure and the crank angle position when the combustion starts. By installing the external chamber, based on the calculation, the peak burned temperature could be reduced around 6.15% compared to the stock engine. Furthermore, according to the temperature graph a constant temperature combustion could be achieved since the equipment restored the energy that has been stored.
3. There are nine parts to assemble the External Chamber. With four of them (Piston 100 mm & 120 mm, Liner 100 mm & 120 mm) are made from Silicon Nitrate Ceramic, while the rest of them are made from aluminum alloy. The external chamber could easily change its size between 100 mm & 120 mm bore by replacing its liner and piston. Lastly, the spring activation pressure can be simply adjusted by rotating the spring compressor into designated position.
4. There are two spring designs, which both of them are designed to handle its own piston sizes. The springs are made from Chrome-vanadium alloy that can handle temperature until 250^{o} C.
5. Based on the calculation, the pipeline will be insulated using a material called calcium silicate, to prevent any excessive heat losses. Since the calculation proves that calcium silicate can saves up to 94.1% of heat energy.

Bibliography:

Wahl, A.M., 1944. Mechanical Spring. The Penton Publishing Company, Cleveland, Ohio.

Spotts, M.F., 1985. Design of Machine Elements. Prentice-Hall of India Private Limited, New Delhi.

Gerhard, S., Dr. Ing. Adamis, P., 1988. Device for Controlling Compression.

Rao, S., 1996. Engineering Optimization: Theory and Practice. 3rd Edn., John Wiley and Sons, New York, ISBN: 0-471-55034-5, pp:858-864.

Carello, M., Ivanov, A., Mazza, L., 1998. Pressure drop in pipe lines for compressed air : comparison between experimental and theoretical analysis. Department of Mechanics - Politecnic di Torino, Torino, Italy.

Fathallah, A.Z.., Bakar, R.., 2010. The Effect of Spring Design as Return Cycle of Two Stroke Spark Ignition Linear Engine on the Combustion Process and Performance. American J. of Engineering and Applied Sciences 3.

Ristiawan, A., Soeprajitno, T., Fathallah, A.Z.., 2013. Desain Pegas pada Motor Bakar Gerak Linier Bersilinder Tunggal dengan Menggunakan Solver. JURNAL TEKNIK SISTEM PERKAPALAN 04.

Hebbar, G.S., 2014. NOx from Diesel Engine Emission and Control Strategies - A Review. International Journal of Mechanical Engineering and Robotics Research.

Fathallah, A.Z.., Semin, Ariana, I.., Gerianto, I., 2014. Motions Study of a Single Cylinder High Speed Spark Ignition Linier Engine with Spring System as Return Cycle. American J. of Engineering and Applied Sciences.

Fitri, S., 2015. Heat Transfer.

Prawira, G., 2018. Development of a Computer Based Combustion Process of a 4 Stroke Diesel Engine and Calculation of Exhaust Gas Emissions for Different Conditions. Hochschule Wismar, Rostock.

Moteki, K., Fujimoto, H., Aoyama, S., n.d. Variable Compression Ratio Mechanism of Reciprocating Internal Combustion Engine. US6505592B2.

Will, F., n.d. Flexibler Pleuel. DE102004000029A1.

Engine Combustion Modeling, n.d.

"This page intentionally left blank"

AUTHOR BIODATA

The author was born on 20th October 1997 in Jakarta, as the second child of 2 siblings. His father's name is Jhonny Lilipaly and his mother's name is Djumiarsih. The author has completed his formal education in Al-Azhar Syifa Budi elementary school, Al-Azhar Syifa Budi junior highschool, and SMAN 1 Tambun Selatan highschool. The author continued his study for bachelor degree in Double Degree Program of Marine Engineering (DDME) of Institut Teknologi Sepuluh Nopember (ITS) and Hochschule Wismar, with student registration number is 04214410000004. During the study, the author took an area of expertise in Marine Power Plant Laboratory (MPP). Furthermore, the author was not only active in academic but also in non-academic activities, such as namely as the staff of Urban Market in ITS Expo 2015 and 2016, senior staff of the ITS Billiard community, and follow some training courses for instances, AutoCAD Basic Training Course, Autodesk Inventor Advanced Course and many more. In addition, the author has been selected to go to Germany to work on his thesis on his last semester. Lastly, the author has done his first on the job training in PT. Bandar Abadi Shipyard, Batam, and his second on the job Training in PT. Medco E&P Natuna Ltd.

Statement of Authorship

I hereby declare that I have prepared and worked on my Bachelor Thesis completely all by myself and have not used any sources or means without any declaration in the text. Any thoughts or literal quotations are clearly marked. This Bachelor Thesis or in similar version have not been used to achieve academic grading or published in other institution.

Rostock, June 2018

Dion Arman Lilipaly

"This page intentionally left blank"

Appendix A

Liner 1 Thermal Expansion simulation (100°C – 500°C)

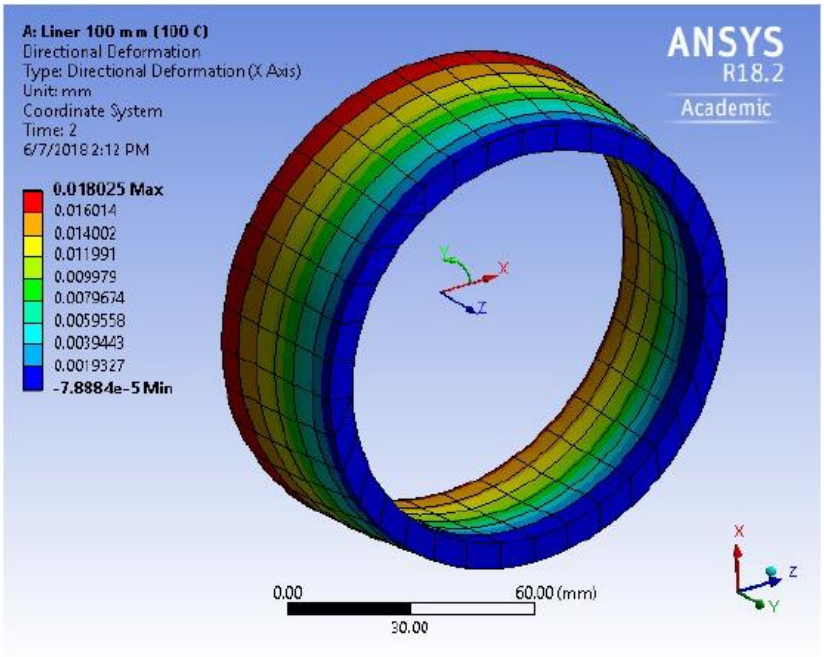

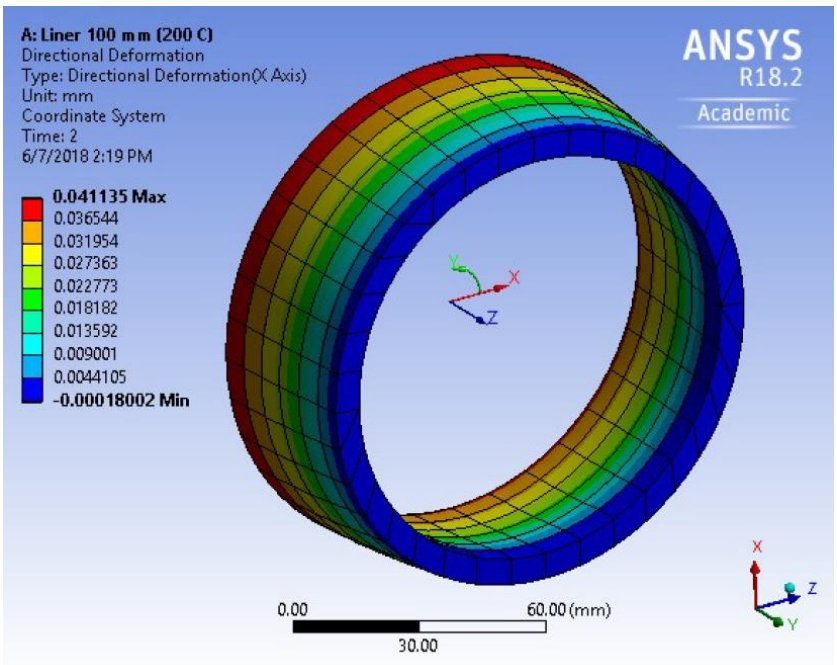

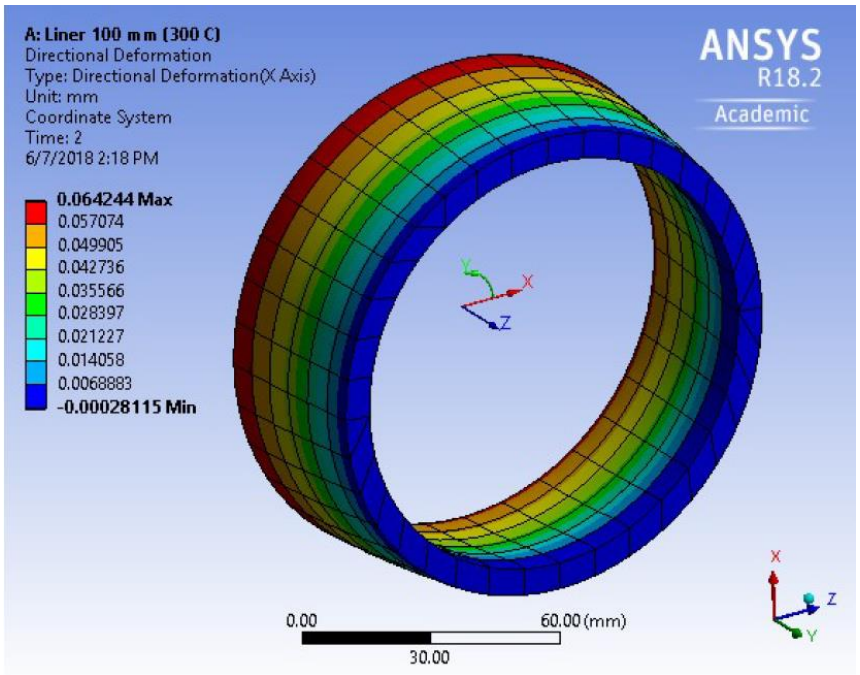
A: Liner 100 mm (300 C)
Directional Deformation
Type: Directional Deformation(X Axis)
Unit: mm
Coordinate System
Time: 2
6/7/2018 2:18 PM
0.064244 Max
0.057074
0.049905
0.042736
0.035566
0.028397
0.021227
0.014058
0.0068883
-0.00028115 Min
ANSYS
R18.2
Academic
0.00
60.00 (mm)
30.00

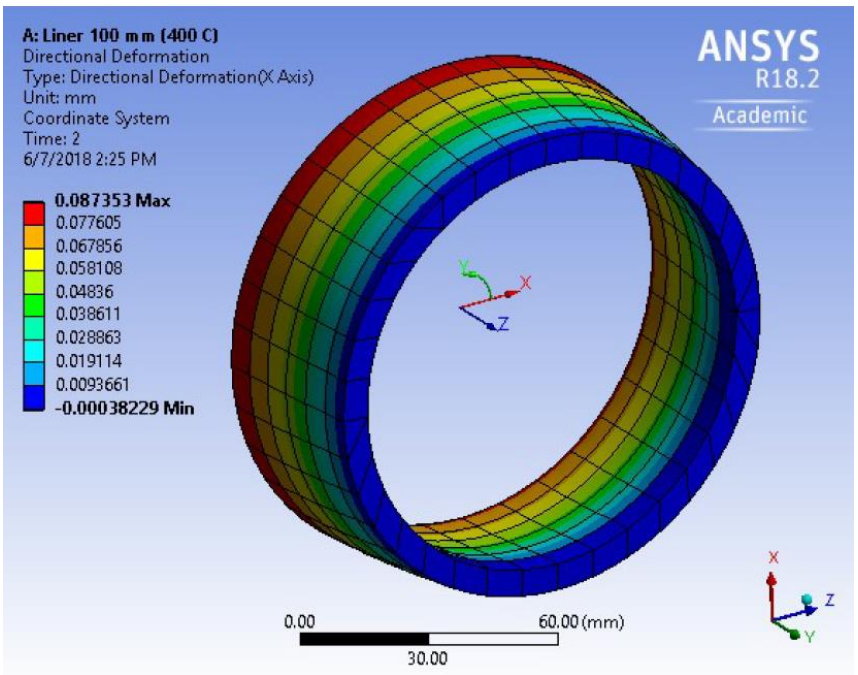
A: Liner 100 mm (400 C)
Directional Deformation
Type: Directional Deformation(X Axis)
Unit: mm
Coordinate System
Time: 2
6/7/2018 2:25 PM
0.087353 Max
0.077605
0.067856
0.058108
0.04836
0.038611
0.028863
0.019114
0.0093661
-0.00038229 Min
ANSYS
R18.2
Academic
0.00
60.00 (mm)
30.00

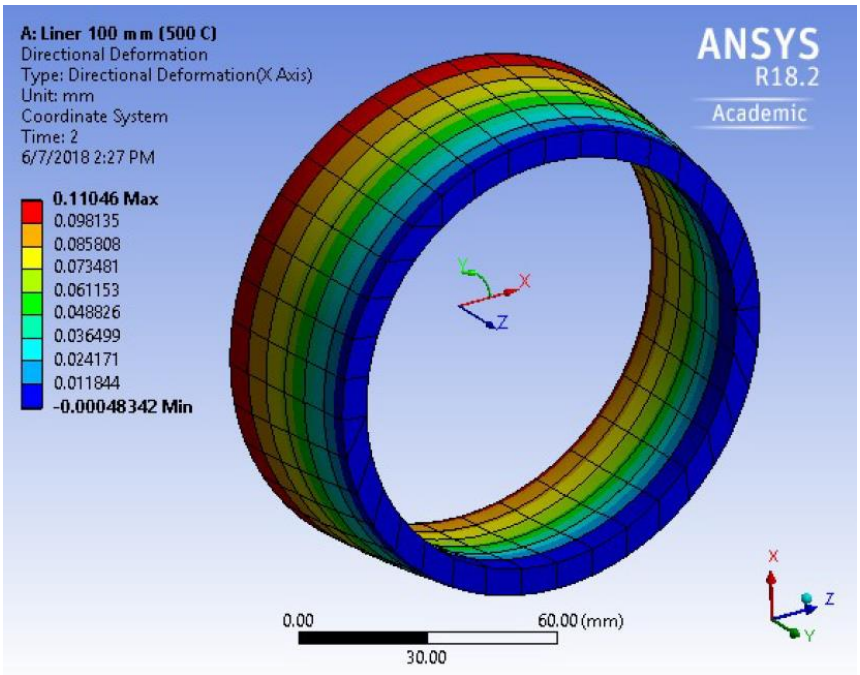
A: Liner 100 mm (500 C)
Directional Deformation
Type: Directional Deformation(X Axis)
Unit: mm
Coordinate System
Time: 2
6/7/2018 2:27 PM
0.11046 Max
0.098135
0.085808
0.073481
0.061153
0.048826
0.036499
0.024171
0.011844
-0.00048342 Min
ANSYS
R18.2
Academic
0.00
60.00 (mm)
30.00

Appendix B

Liner 2 Thermal Expansion simulation (100°C – 500°C)

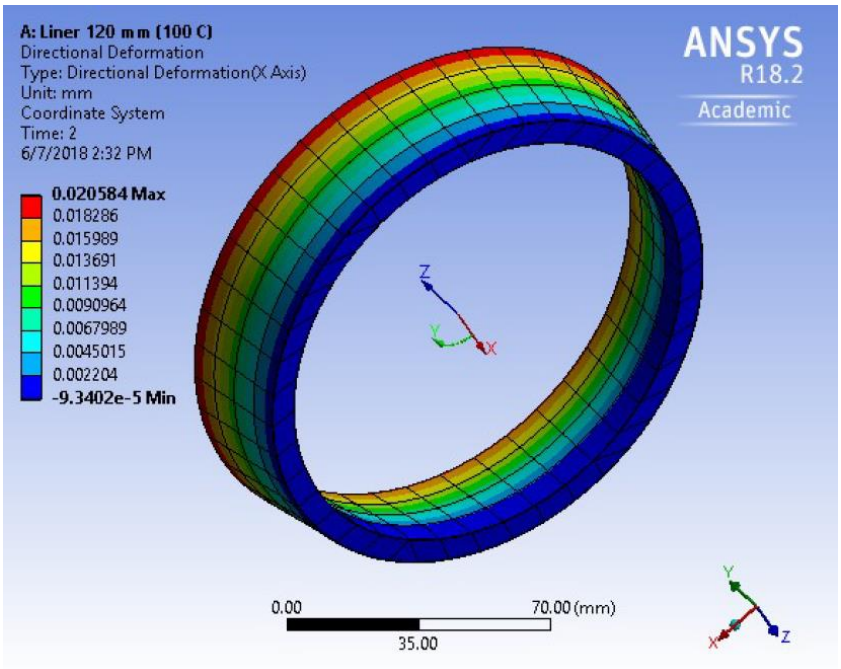

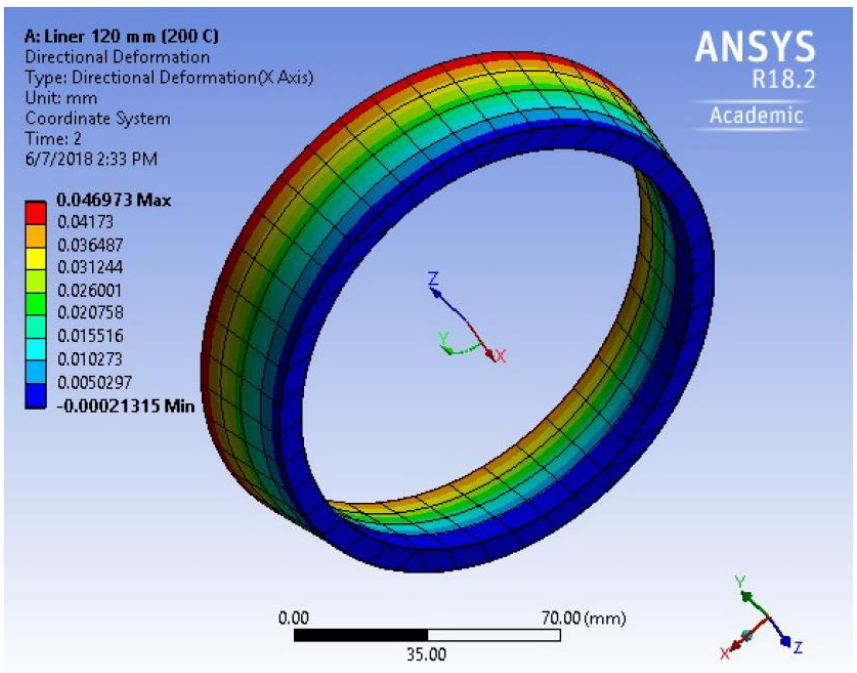

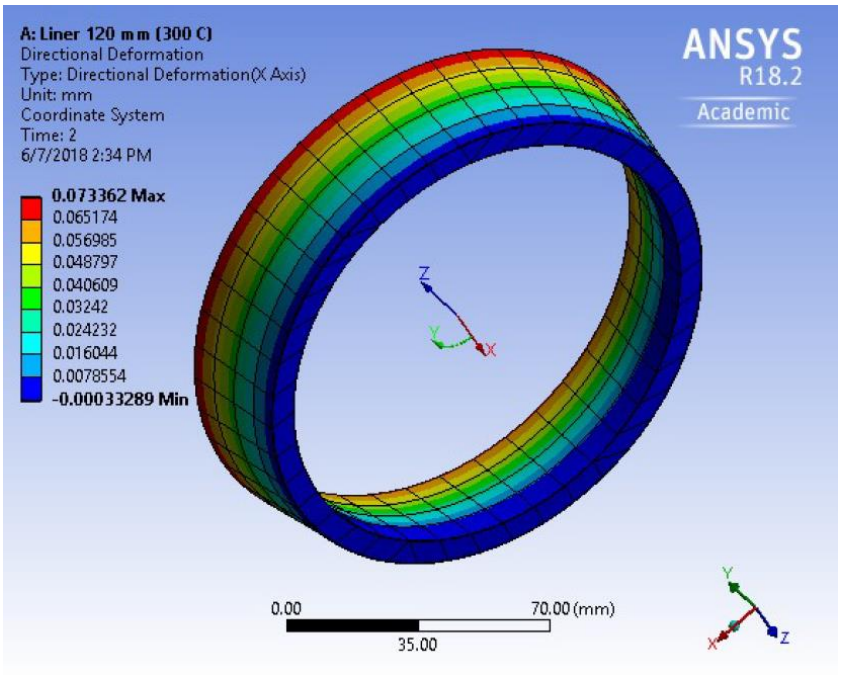
A: Liner 120 mm (300 C)
Directional Deformation
Type: Directional Deformation(X Axis)
Unit: mm
Coordinate System
Time: 2
6/7/2018 2:34 PM
0.073362 Max
0.065174
0.056985
0.048797
0.040609
0.03242
0.024232
0.016044
0.0078554
-0.00033289 Min
ANSYS
R18.2
Academic
0.00
70.00 (mm)
35.00

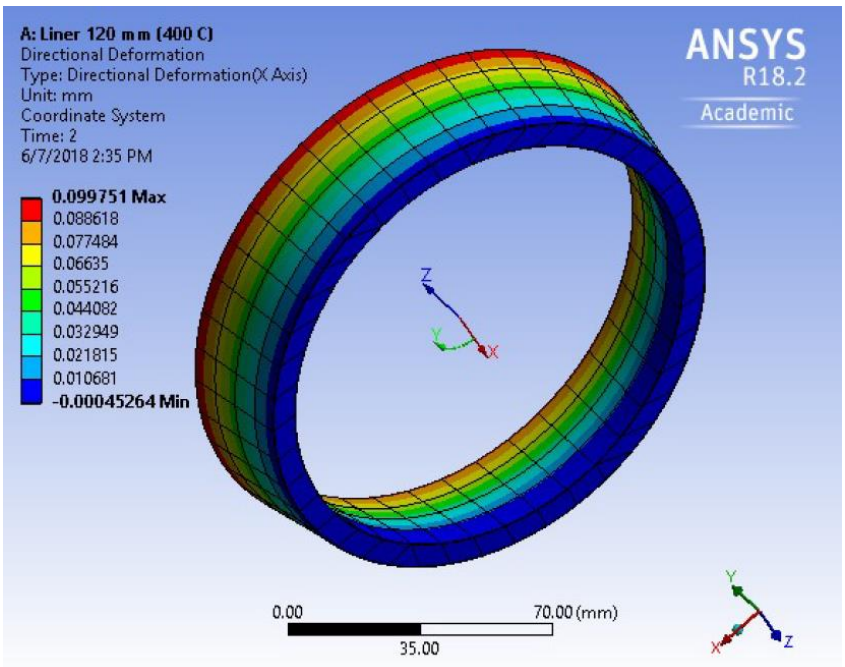
A: Liner 120 mm (400 C)
Directional Deformation
Type: Directional Deformation(X Axis)
Unit: mm
Coordinate System
Time: 2
6/7/2018 2:35 PM
0.099751 Max
0.088618
0.077484
0.06635
0.055216
0.044082
0.032949
0.021815
0.010681
-0.00045264 Min
ANSYS
R18.2
Academic
0.00
70.00 (mm)
35.00

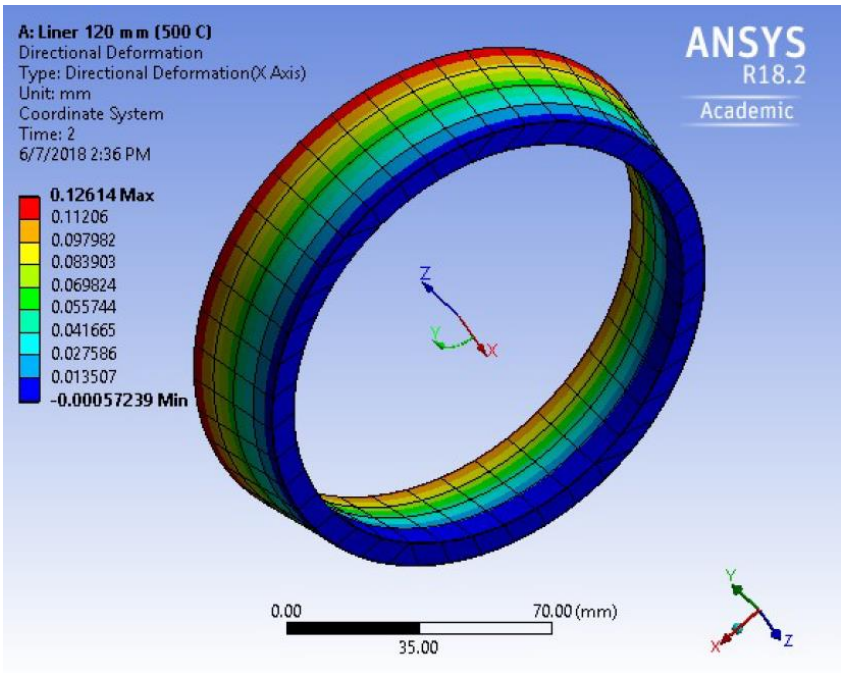
A: Liner 120 mm (500 C)
Directional Deformation
Type: Directional Deformation(X Axis)
Unit: mm
Coordinate System
Time: 2
6/7/2018 2:36 PM
0.12614 Max
0.11206
0.097982
0.083903
0.069824
0.055744
0.041665
0.027586
0.013507
-0.00057239 Min
ANSYS
R18.2
Academic
0.00
70.00 (mm)
35.00
Z
Y
X

Appendix C

1. Spring 1 Dimension
2. Spring 2 Dimension
3. Secondary Chamber Exploded View

Top View

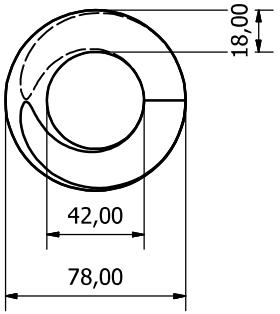

Front View

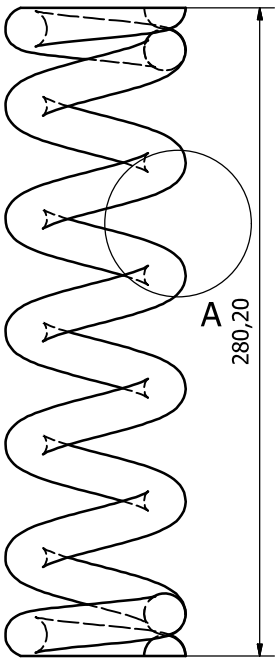

Side View

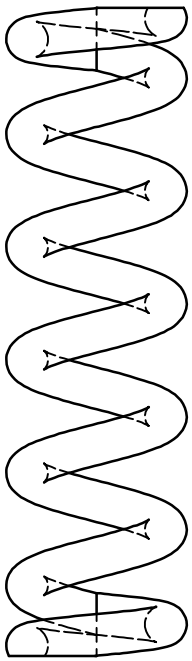

Isometric View

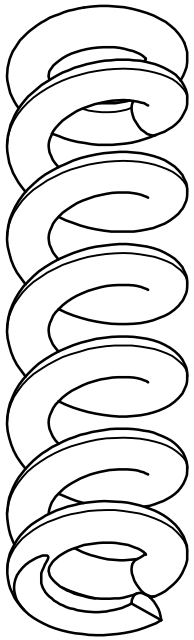

A (1 : 1)

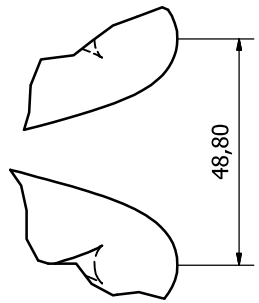

Compression Spring		
Number of active coil	n	5
Inactive coil	n'	2
Coil end		Squared Ground End
Direction of coil winding		Right
Spring constant [N/mm]	k	953.775
Spring weight [kg]	m	2.686
Outer spring diameter	De	78
Inner spring diameter	Di	42
Free spring length	LO	280
Preloaded spring length	L1	222.358
Fully loaded spring length	L8	189.748
Theoritic spring limit length	Ls	126
Minimum working loading [N]	F1	54977.9
Maximum working loading [N]	F8	86079.6
Theoritic spring limit loading [N]	Fs	146881
Spring material :		
Chrome-vanadium alloy steel wire JIS SUP 10		
Wire diameter	d	18

Designed by	Checked by	Approved by	Date	Date	
Dion Arman Lilipaly				5/7/2018	

Hochschule Wismar	Spring Specification		
	100 mm Spring Free Length	Edition	Sheet 1 / 1

C (1 : 1)

Top View

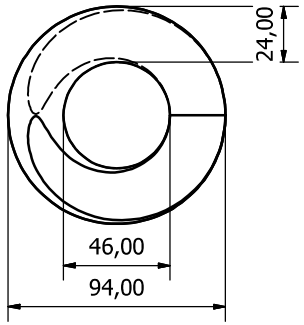

Front View

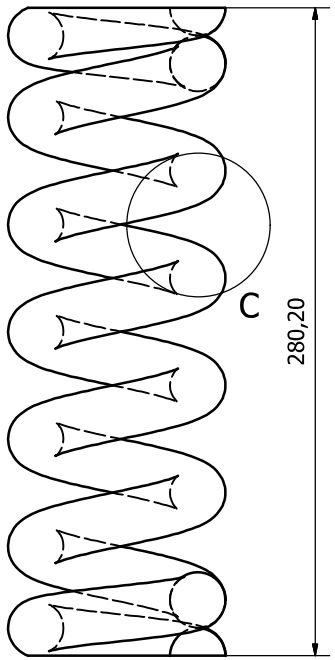

Side View

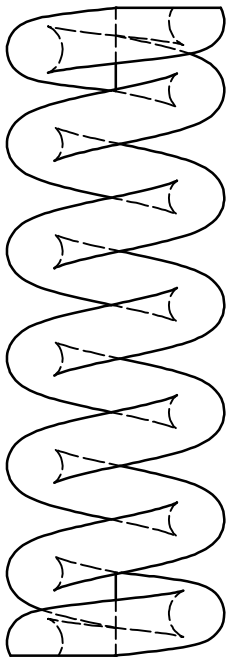

Isometric View

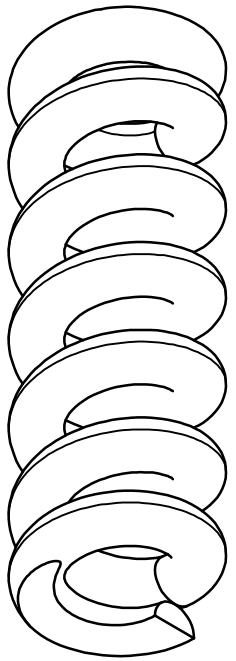

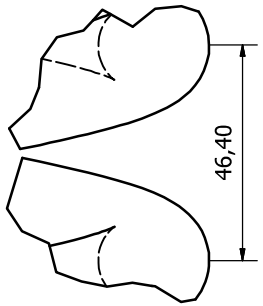

Compression Spring		
Number of active coil	n	5
Inactive coil	n'	2
Coil end		Squared Ground End
Direction of coil winding		Right
Spring constant [N/mm]	k	1898.28
Spring weight [kg]	m	5.571
Outer spring diameter	De	94
Inner spring diameter	Di	46
Free spring length	LO	280
Preloaded spring length	L1	238.3
Fully loaded spring length	L8	214.7
Theoritic spring limit length	Ls	168
Minimum working loading [N]	F1	79168.1
Maximum working loading [N]	F8	123955
Theoritic spring limit loading [N]	Fs	212607.48
Spring material :		
Chrome-vanadium alloy steel wire JIS SUP 10		
Wire diameter	d	21

Designed by	Checked by	Approved by	Date	Date	
Dion Arman Lilipaly				5/7/2018	

Hochshule Wismar	Spring for 120 mm bore		
	120 mm Spring Free Length	Edition	Sheet 1 / 1

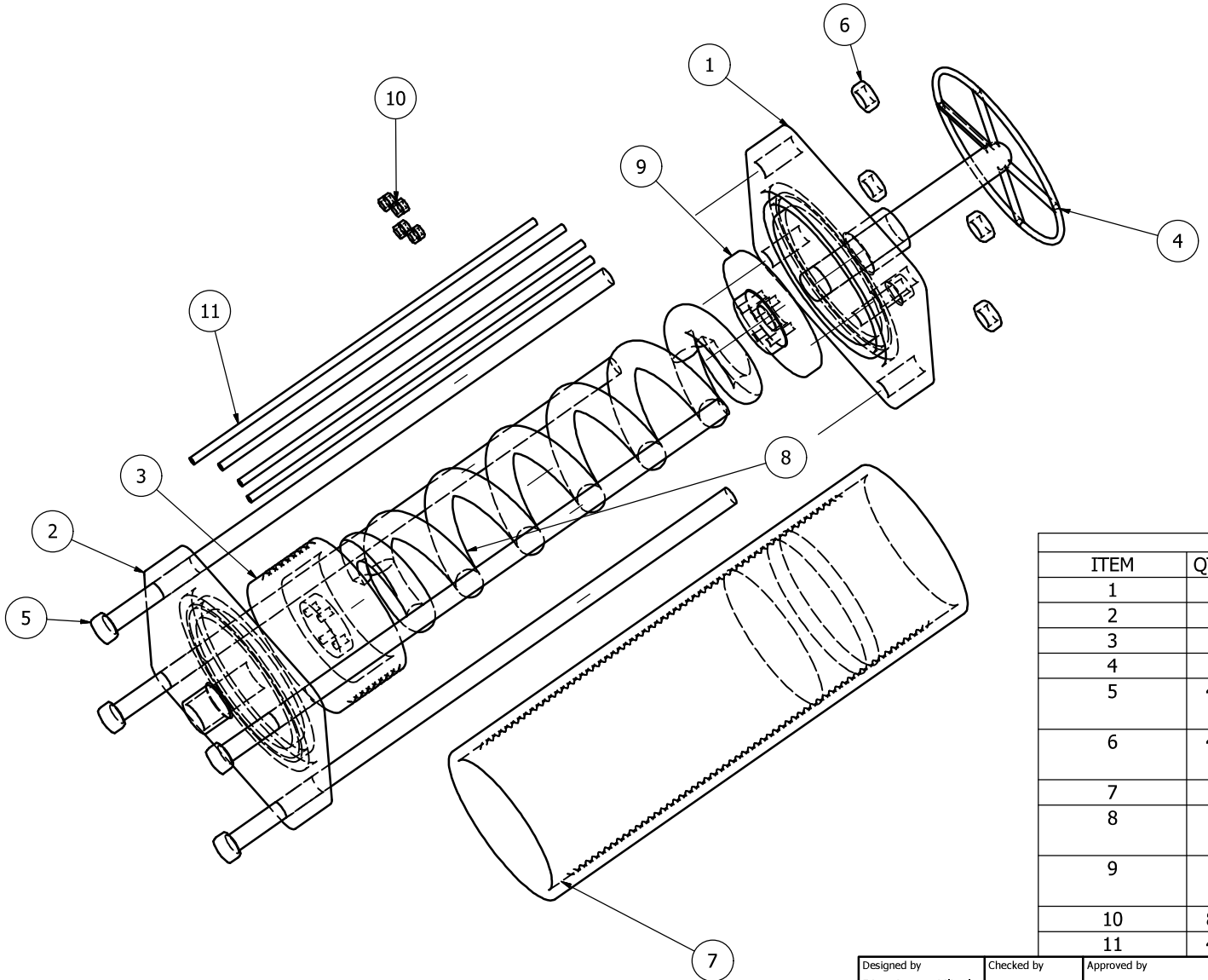

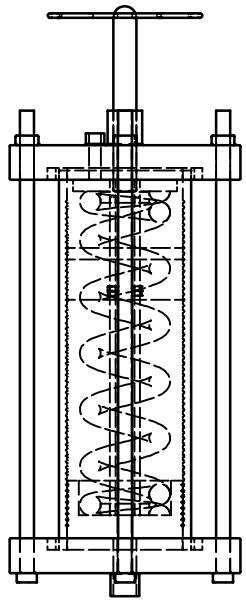

PARTS LIST			
ITEM	QTY	PART NUMBER	DESCRIPTION
1	1	Top	
2	1	Bottom	
3	1	Piston 100mm	
4	1	Handle	
5	4	20 mm bolts (12 mm hole)	
6	4	nuts 20 mm (hole 12 mm)	
7	1	Liner 100 mm	
8	1	Spring Free Length	
9	1	100 mm Spring Seater	
10	8	Nuts Stopper	
11	4	Stopper	

Designed by	Checked by	Approved by	Date	Date
Dion Arman Lilipaly				6/6/2018

Hochschule Wismar	External Chamber		
	External Chamber	Edition 01	Sheet 1 / 1